An investigation of the Felsic Ramiane Pluton, in the Monapo Structure, Northern Moçambique

Jonnina P. Karlsson

Examensarbeten i Geologi vid
Lunds universitet - Berggrundsgeologi, nr. 202

Geologiska institutionen
Centrum för GeoBiosfärsvetenskap
Lunds universitet
2006

AN INVESTIGATION OF THE FELSIC RAMIANE PLUTON, IN THE MONAPO STRUCTURE, NORTHERN MOÇAMBIQUE

JONNINA P. KARLSSON

Karlsson, J. P., 2006: An investigation of the Felsic Ramiane Pluton in the Monapo Structure, Northern Moçambique. M.Sc. Thesis in Geology at the University of Lund. Nr. 202.

Abstract

The Monapo Structure is situated in the Nampula Subprovince in northern Moçambique, and makes up a part of the Moçambique Orogenic Belt. It is a 35 x 40 km subcircular structure, with a very flat topography, and it clearly shows up on aerial photos. The regional setting of the Monapo Structure is not yet clearly settled and many questions regarding transportation directions, lithostratigraphic groupings and tectonic setting of the area are still under debate.

The Ramiane Pluton is situated in the eastern parts of the Monapo Structure and makes up a large part of the felsic, A-type, Ramiane Suite. The pluton comprises mostly alkaline granites, but other rock types also exist. Petrographic studies have shown fluid inclusions in garnet and quartz from the pluton, and hence indicate that the pluton was rich in fluids when emplaced. The almandine-andradite rich garnet is concentrated in leucocratic patches, interpreted as fluid-rich areas, where biotite, amphibole and oxides are clearly absent. This has been interpreted as a retrograde process due to increased $fO2$. Calculations of P and T have yielded results that show large variations that are dependent on the water activity and the presence or absence of fluids. Nevertheless, the P-T's indicate that the pluton intruded at granulite-facies conditions. Modelling of a possible protolith of the Ramiane has indicated a relatively juvenile protolith that does not appear to be related to either the rocks of the Nampula Subprovince or those of the Monapo structure. SHRIMP U-Pb data from zircons have yielded an intrusive event at 636.8 ± 5.3 Ma as well as a younger age of 596 ± 5 Ma. Both these ages are within the Pan-African time span. However, these ages are very similar to those obtained on the Metacheria basement rocks, which are thought to pre-date the Ramiane. The lithostratigraphic relationship between the Ramiane and the Metacheria basement are thus unsettled. Further studies on the Metacheria basement are needed in order to resolve this question

Keywords; Moçambique Orogenic Belt, Nampula Subprovince, Monapo Structure, Ramiane Pluton.

Jonnina P. Karlsson, Department of Geology, Geobiosphere Science Centre, the University of Lund, Sölvegatan 12, 223 62 Lund, Sweden.

UNDERSÖKNING AV DEN FELSISKA RAMIANE PLUTONEN I MONAPO STRUKTUREN, NORRA MOÇAMBIQUE.

JONNINA P. KARLSSON

Sammanfattning

Monapostrukturen ligger i Nampula provinsen i norra Moçambique, och utgör en del av Mocambique bältet. Strukturen är ca 35-40 km i diameter och har en mycket låg topografi. Trots detta syns den väl på satellitbilder och flygfotografier. Relationer mellan samt utbredning av de enskilda bergartsleden är inte helt klarlagd och frågor såsom transportriktning, litostratigrafisk uppdelning samt tektonisk miljö debatteras fortfarande.

Ramianeplutonen ligger i de östra delarna av Monapostrukturen, och utgör en stor del av den felsiska, A-typ, Ramianegruppen. Plutonen består till mesta del av alkalina graniter, men det finns även andra bergarter representerade. Petrografi har påvisat vätskeinklusioner i granat och kvarts från plutonen. Detta indikerar därmed att det troligen rör sig om en pluton som var vätskerik vid intrusionen. Den almandin-andradit rika granaten i plutonen är i stor utsträckning koncentrerad till leukokratiska områden i bergarten. Kristalliseringen av granat har tolkats som en retrograd process som ägt rum vid ökad f_{O2}. Kemiska analyser på de olika mineralen i bergarten visar att den intrusiva temperaturen och trycket för plutonen har varit höga. Tryck och temperatur vid bildandet av granat har blivit beräknade och visar relativt stora skillnader beroende på vatten aktiviteten i plutonen, samt om plutonen var vätskerik eller vätskefattig. Modellerande av en möjlig protolit till Ramianeplutonen indikerar en juvenil protolit som inte verkar vara besläktad med vare sig bergarter från Nampula provinsen eller från Monapostrukturen. SHRIMP U-Pb dateringar av zirkoner rån Ramianeplutonen har gett en intrusiv ålder på 636.8 ± 5.3 Ma samt en yngre ålder på 596 ± 5 Ma. Båda dessa åldrar faller inom det Pan-afrikanska åldersspannet. De är även mycket lika åldrarna från Metacheriakomplexet som Ramianeplutonen tros ha intruderat i. För att bestämma de två bergarternas relation till varandra måste mer forskning utföras på Metacheria komplexet.

Nyckelord: Moçambique bältet, Nampula provinsen, Monapostrukturen, Ramianeplutonen.

Jonnina P. Karlsson, Geologiska institutionen, centrum för GeoBiosfärsvetenskap, Lunds universitet, Sölvegatan 12, 223 62 Lund, Sverige.

TABLE OF CONTENTS

1. INTRODUCTION **5**

1.1. Introduction **5**

1.2. Aims of this study **7**

1.3. Methodology and Approach **7**

2. REGIONAL GEOLOGY **8**

2.1. Introduction **8**

2.2. Location of study area **9**

2.3. The Supercontinents and the Moçambique Belt **9**

2.4. Geology of northern Moçambique **11**

2.5. The Monapo Structure **11**

2.5.1. Stratigraphy 11

2.5.2. Structure 13

2.5.3. Geochronology 14

3. PETROLOGY AND MINERAL CHEMISTRY **14**

3.1. Petrology **14**

3.2. Mineral Chemistry **18**

3.2.1. Feldspars 18

3.2.2. Garnet 18

3.2.3. Amphibole 20

3.2.4. Biotite 20

4. GEOCHEMISTRY AND STABLE ISOTOPES **20**

4.1. Whole rock geochemistry **20**

4.1.1. Major elements 20

4.1.2. Trace elements 21

4.1.3. Rare earth elements 25

4.2. Stable isotopes **26**

5. DISCUSSION **26**

5.1. Petrology and Mineral chemistry **26**

5.2. P-T- modelling **28**

5.3. Possible protolith and its mechanical evolution **29**

5.4. Geochronology **32**

6. CONCLUSIONS **33**

7. ACKNOWLEDGEMENTS **34**

8. LIST OF REFERENCES **35**

9. APPENDIX

1. INTRODUCTION

1.1. Introduction

The Monapo Structure is situated in northern Moçambique (Fig. 1). From the air it is a clearly visible subcircular geological feature, with dimensions of 40 by 35 km. In general it is composed of a series of alkaline, ultramafic and felsic rocks intruding into granulite-facies basement rocks. The Monapo Structure has been a source of geological interest for many years due to its economic apatite deposits. However, a recent World Bank sponsored mapping project in Moçambique has brought to attention the possible role of the Monapo Structure in unravelling the tectonic evolution of northern Moçambique.

The Monapo Structure has a complicated geological history that has been the subject of much debate. At the centre of this debate, is the issue of whether the Monapo Structure represents a klippe or a window. Most previous studies have connected the Monapo Structure with the granulitic Ocua (formerly referred to as Lurio) rocks to the north and have thus interpreted the Monapo Structure to be a part of a southward-directed thrust sheet. This would imply that the surrounding area has eroded and left the Monapo as a remnant of an original allochthonous nappe. In addition to the Monapo Structure there are also at least two more geological remnants in northern Moçambique connected with the same possible Pan-African thrusting event, the Mugeba and the Plantação klippes. However out of these three geological features, there are only alkaline intrusive rocks in the Monapo Structure, which in turn could imply a more complex history to the Monapo Structure than that of the other assumed klippes. There may also be a connection in time and

Figure 1. Overview of southern Africa, with Moçambique and the location of the Monapo Structure in northern Moçambique. Eye altitude and width of picture are both approximately 4500 km.

Figure 2. The 40 x 35 km alkaline Monapo Structure situated approximately 50 kilometres from the Indian Ocean.

event to granulitic rocks on Sri Lanka. Such a connection needs further investigation and is not within the scope of this thesis.

The other model is that the Monapo Structure represents a window, possibly into a large scale recumbent fold created due to thrusting. This thrusting event may have occurred in the middle or lower crust which would explain the high metamorphic grade of the surrounding rocks. One way of solving the issue of the contrasting klippe/ window models is to try to determine if the intrusive rocks were intruded *in situ* or not. Such information would help to resolve whether the Monapo structure is allochthonous or autochthonous and consequently if it is a klippe or not.

Our knowledge of the Monapo Structure is at the moment very limited and that is one of the reasons for the uncertainties regarding its nature. By investigating the felsic Ramiane Pluton of the Ramiane Suite, I hope to add more information to our understanding of the Monapo Structure (Fig. 2).

The whole rock chemistry of the Ramiane Pluton can indicate the nature of the protolith and that together with the SHRIMP data can give an indication of whether the Ramiane Pluton and the Monapo Structure is connected to the large scale Pan-African event or not. By collecting and analysing whole rock chemistry and stable isotope data from the structure and compare them to surrounding rocks, constraints on the structure and its evolution can be made. The whole rock chemistry for example, can classify the Ramiane Pluton rocks and the stable isotopes may give results that will yield additional information about the origin of these felsic rocks, such as if it is an I- or S-type granite. Comparisons with the other assumed klippes in the area could then give an answer to if the Monapo Structure is related to them or not. If the rocks in the structure are not similar in composition and origin to the other two klippes it would appear as if they are not closely related and thus have different origins and geological evolutions.

By investigating the petrogenesis of several different rock types in the structure, modelling can be made and mechanisms that controlled the rock evolution and composition investigated (e.g. Martin, 1987). The modelled results may then help to understand the evolution of

the Monapo Structure in the sense that it may reveal if it has a protolith originating from the surrounding Metacheria Complex or Nampula Subprovince rock types or not. Also, it can possibly tell us if the rock is highly evolved or not. Again, these results can be compared to the rocks north of the Lurio Belt as well as the other assumed klippes.

The possible pressure (P) and temperature (T) conditions that can be calculated after mineral chemistry analyses has been carried out, may give an idea to under what P and T circumstances the Ramiane Pluton intruded and/ or metamorphosed. This may also bring to attention the possible tectonic setting of the area, which can be determined to a certain extent with the help of P and T.

1.2. Aims of this study

The primary objective of this thesis is to investigate the nature of the Ramiane Pluton of the Ramiane Suite and in doing so add to our understanding of the Monapo Structure. The specific aims of the project are as follows;

Aim 1: To classify the Ramiane Plutonic rocks and determine whether they are granitic or syenitic, alkaline or calc-alkaline etc, in composition.

Aim 2: To create an understanding of whether all the features in the Ramiane Pluton are primary, ie igneous, or secondary, ie metamorphic.

Aim 3: To determine the P-T conditions of the intrusive and/ or metamorphic event and the timing of development of the garnet-bearing patches.

Aim 4: To determine the intrusive age of the Ramiane Pluton and the timing of the metamorphic overprint.

Aim 5: To determine via modelling what is a viable source rock composition as well as its possible mechanical evolution, and investigate if anything in the region appears to be the protolith.

Aim 6: To compile the above information into a model for the evolution of the Ramiane Pluton and its relevance to the Monapo Structure.

1.3. Methodology and Approach

The rock samples were collected from two separate fieldtrips during 2004 and 2005 by Dr. Paul Macey and Dr. Jodie Miller. The samples from 2005 were analysed at Stellenbosch University during 2006 as part of this thesis, while the samples from 2004 were analysed at a different location during 2005. Samples JM05MC-21 and JM05MC-22 represent areas of finer grained varieties of the pluton, while all the others represent more coarse grained localities. Sample JM05MC-19 represents a locality with homogenous host rock as well as garnet bearing leucocratic patches, hence JM05MC-19 is divided into JM05MC-19 and JM05MC-19B. Sample JM05MC-19 is a garnet bearing leucocratic patch while JM05MC-19B is from the more homogenous host rock.

The whole rock chemistry samples were split and crushed by hand, and afterwards milled in a swing mill before being prepared for XRF analyses. Major element and trace element analyses were made by XRFS, X-Ray Fluorescence Spectrometry, on a Philips 1404 Wavelength Dispersive spectrometer. The spectrometer has a built in Rh tube and six analysing crystals. Major elements were analysed on fused glass beads and trace elements were analysed on powder briquettes with the XRFS operating at 50 kV, 50 mA and 60 kV, 40 mA respectively. Matrix effects were corrected for online and the instrument was calibrated against a range of international standards.

Rare earth elements were analysed with LA

ICP-MS, Laser Ablation Inductively Coupled Plasma-Mass Spectrometry. The pulse rate was 20 Hz and each spot had an analysing time of 38 seconds. The spot size was 80 μm, and an average value from three spots/ sample was used. The silica values received from previously made XRF analyses were used for the internal calibration and the standards NIST 614 and NIST 612 were analysed at the same time as the samples. The La values from the ICP-MS are unusually high and this could possibly be due to La contamination of the fuse bead flux. However, the sample batch from 2004 also shows a high La value, although not as high as the ones from 2005.

The REE_{tot} values from the batch of 2004 vary from the ones from 2005 in that they have more trace elements and less rare earth elements analysed and hence the 2004 samples are not included in the REE_{tot} in this thesis. However, they are represented in the multi-element and REE diagrams.

BSE imaging and mineral chemistry analyses were carried out on thinsections that were polished and carbon coated before being analysed. The analyses were carried out using a Leo® 1430VP Scanning Electron Microscope. The mineral compositions were quantified by EDS analysis using an Oxford Instruments® 133KeV detector and Oxford INCA software. The beam current was 3.92 nA and the working distance approximately 13 mm. The time for data collection was 50 seconds.

Stable isotope data was collected at the University of Cape Town, UCT. The rocks used for whole rock stable isotope collection, were split and crushed by hand, and afterwards milled in a swing mill. The sieving for the mineral picking was made with the 710μ, 550μ and 300μ sieves. Quartz was then hand picked, and crushed by hand with an agate mortar and pestle. Sample JM05MC-22 appeared to have too many inclusions and hence was not used in the quartz stable isotope analysis. The oxygen isotope ratios were determined by conventional fluorination methods (Clayton and Mayeda, 1963) using ClF_3 as the oxidising reagent (Borthwick and Harmon, 1982). Samples reacted overnight at 550 ºC. After conversion to CO_2, isotope ratios were determined on a Finnigan MAT 252 mass spectrometer housed in the Department of Archaeology at UCT. Data were reported in δ where $\delta^{18}O$ is $(R_{sample}/R_{standard} - 1) \times 10^3$ ‰ and R is the ratio of $^{18}O/^{16}O$. A quartz standard (MQ) calibrated against NBS-28 was analysed in duplicate with each run of eight samples and used to convert the raw data to the SMOW (Standard Mean Ocean Water) scale using the value of 9.64% for NBS-28 recommended by Coplen *et al.* (1983). The average observed difference between MQ duplicates during the course of this work was 0.09 ‰ (n = 8).

Concordia age for rock sample JM05MC-19 was obtained on zircons using SHRIMP U-Pb data. Analysis carried out at the Australian National University, for the Council for Geosciences in Pretoria. All of the geochronology data in the Geochronology section are provided by the CGS, Council for Geosciences, in South Africa and are at present unpublished if not otherwise indicated.

2. REGIONAL GEOLOGY

2.1. Introduction

The Monapo Structure is situated in northern Moçambique, and forms part of the Moçambique Orogenic Belt. This orogenic belt runs along the eastern part of the African continent, from the southern parts of Moçambique via Tanzania, Kenya, Ethiopia and Sudan and onwards towards Egypt. It is considered to represent an important

Figure 3. View over the Ramiane sisal plantation illustrating the flat topography of the area.

site of both rifting and suturing during both the break-up of Rodinia and the assembly and break-up of Gondwana. I will here discuss the known regional geology of the Monapo structure and how it relates to the regional geology of the Moçambique Belt.

The geological knowledge of the area is at the moment quite limited. However, due to a World Bank sponsored mapping project in the area, large quantities of data are about to become available and as a result of that the description of the regional geology given in this thesis may have to be revised in the near future. The terminology used by the different groups involved in the World Bank project for northern Moçambique is occasionally confusing and problematic due to different interpretations. Some use tectonostratigraphic terms and some use lithostratigraphic terms. For example the Nampula is named a Subprovince by the CGS and a Complex by the NGU, Norges Geologiske Undersøkelse. In this thesis the terminology of the CGS will be used.

2.2. Location of study area

The Monapo Structure is located between latitudes 14° 37' S-15° 02' S and longitudes 39° 55' E- 40° 19' E, in the eastern Nampula Subprovince, approximately 50 kilometres from the Indian Ocean. The structure is situated in an agricultural area dominated by plantations of sisal and cashew nuts (Fig. 3).

The structure is a flat geological feature with a few minor hills. The Ramiane Pluton, which is the object of this thesis, has been named after the Ramiane sisal plantation where it crops out (Fig. 4).

2.3. The Supercontinents and the Moçambique Belt

The Moçambique Belt has a long and complicated history, and the extent of the belt is not always easy to determine. It has been activated and reworked at least twice during its history, and as a result the northern and southern boundaries of the belt are not clearly outlined. The boundary to the north has been strongly affected by Pan-African tectonism (Pinna *et al*, 1993), and the location of the boundary to the south is still under debate (Grantham *et al,* 2003).

The Moçambique Belt was first thought to be a completely Pan-African structure because

Figure 4. View towards one of the minor Ramiane Pluton ridges.

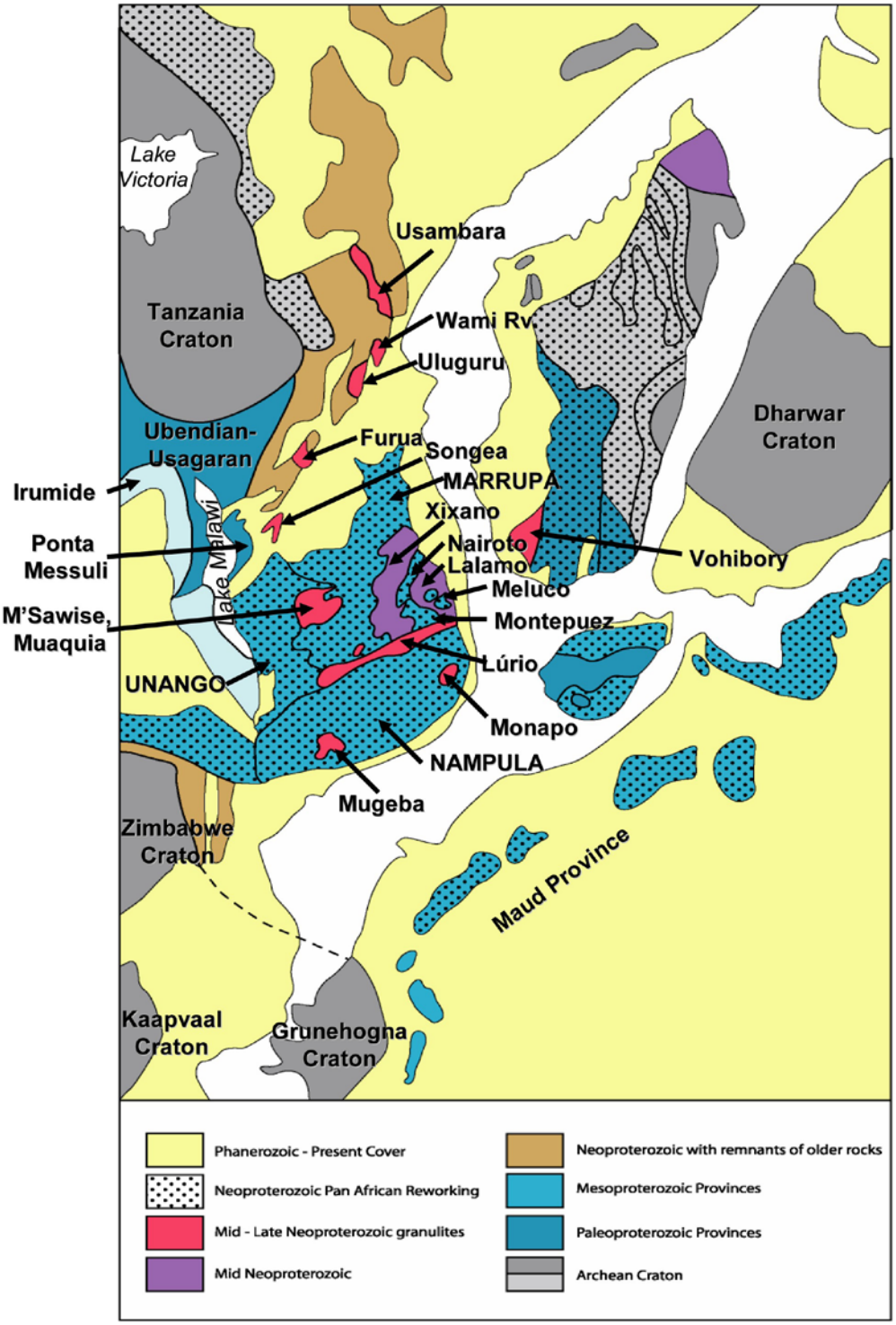

Figure 5. Overview of the different terranes in northern Moçambique, with one of the suggested cratonic assemblages of the area during the Pan-African amalgamation of Gondwana. The possible correlationship between the Nampula, the Marrupa, Sri Lanka and provinces in Antarctica is clearly visible on the map. Mid- Late Neoproterozoic granulitic areas such as the Monapo and the Mugeba appears as red areas, while dark blue areas represent Paleoproterozoic provinces and the light blue areas represent Mesoproterozoic provinces. The reworking overprint of the Pan-African event is apparent in a large part of the map.

of the many ages obtained around 600-500 Ma (Grantham *et al*, 2003). However, continued research has shown that these ages were metamorphic cooling ages of the rocks. In most locations the crystallization ages indicated dates of 1200-1000 Ma, the Kibaran age (Grantham *et al*, 2003). These 1200-1000 Ma dates are associated with the amalgamation of the supercontinent Rodinia during a period of extensive plate tectonic activity (Grantham *et al*, 2003). The extensive plate tectonism at that time is evident in the subsequent formation of the Grenvillian (North America), Sveconorwegian (Europe), Kibaran, Iremide and Namaqua-Natal (Africa), Albany-Fraser (Australia) and the Rodinia-Sunsas (South America) Orogenic Belts (Groenwald *et al*, 1995). Several ages between 800-700 Ma have also been obtained from

the Moçambique Belt. These ages are thought to represent the break-up of Rodinia and the subsequent openings of the Moçambique and Adamastor Oceans (Grantham *et al*, 2003). Still younger ages, between 600 and 480 Ma, reflect the reworking of the Kibaran aged rocks during the Pan-African Orogeny. These younger ages, as well as the amalgamation of Gondwana are supported by palaeomagnetic data which shows apparent polar wander paths coming together at approximately 550 Ma (Kröner, 1991).

The terrains of the Moçambique Belt are mostly high grade metamorphic terrains with rock types such as granulite, high grade gneisses and migmatites (Pinna *et al*, 1993). There is also evidence of smaller, intrusive alkaline complexes at different localities, such as the Monapo Structure as well as in the Lurio Belt region. Occasionally there is evidence of volcanoclastic terrains (Macey *et al*, 2006).

2.4. Geology of northern Moçambique

Together with several complexes, the Nampula Subprovince, which are the host rocks to the Monapo Structure, makes up a part of the northern Moçambiquan Mesoproterozoic geology (Fig. 5). The Nampula Subprovince is separated from the Marrupa and the Montepuez Complexes to the north by the Pan-African Lurio Belt. Former studies have shown that the granulitic Lurio Belt was a Pan-African suture related structure (Sacchi *et al*, 2000). However, more recent studies have pointed out that the Lurio Belt does not always represent a distinct break in lithologies between the northern Marrupa and Montepuez Complexes, and the southern Nampula Subprovince (Viola *et al*, 2006) As a result, the Pan-African suture zone model has been called into question (Viola *et al*, 2006). Additionally, structural features along the belt are quite variable. They change from the eastern Montepuez region to the western Ribaue-Malema region, in that the concentration of linear features become broader and not as "belt like" (Viola *et al*, 2006). Nevertheless, there are also important similarities within the Lurio Belt, such as the dips of the axial planes and the plunge axes. However, the Lurio Belt might not be entirely Pan-African. Some Lurio Belt rocks have yielded older ages and it is possible that the Nampula Subprovince docked on the northern landmass during the Kibaran. The evidence for this is the occurrence of zircons dated at 1127 Ma in both Antarctica and the Nampula Subprovince, but not north of the Lurio Belt.

Lithologically, the Nampula Subprovince consists of medium- to upper-amphibolite facies gneisses of Mesoproterozoic origin that were intruded by younger Pan-African pegmatoids and granites. The oldest rocks in the area are the tonalitic-trondhjemitic-granodioritic Mocuba orthogneisses, with an age of c.1125 Ma (unpublished U-Pb SHRIMP zircon data, Macey and Armstrong). Other Mesoproterozoic rocks in the area include the Moloque Group, the Culicui Suite, the Mamala Formation and the Rapale Gneiss. The younger Pan-African plutons and dykes that intruded into these Mesoproterozoic rocks make up the Murrupula Suite. Inselbergs from the Culicui Suite are common features in the Nampula Subprovince but they do not occur in the Monapo Structure itself.

2.5. The Monapo Structure

2.5.1. Stratigraphy

The lithostratigraphy of the Monapo Structure is separated into three main groups; 1) the Metacheria Metamorphic Complex; 2) the intrusive Mazerapane and Ramiane Suites; and 3) rocks with similar composition to those of

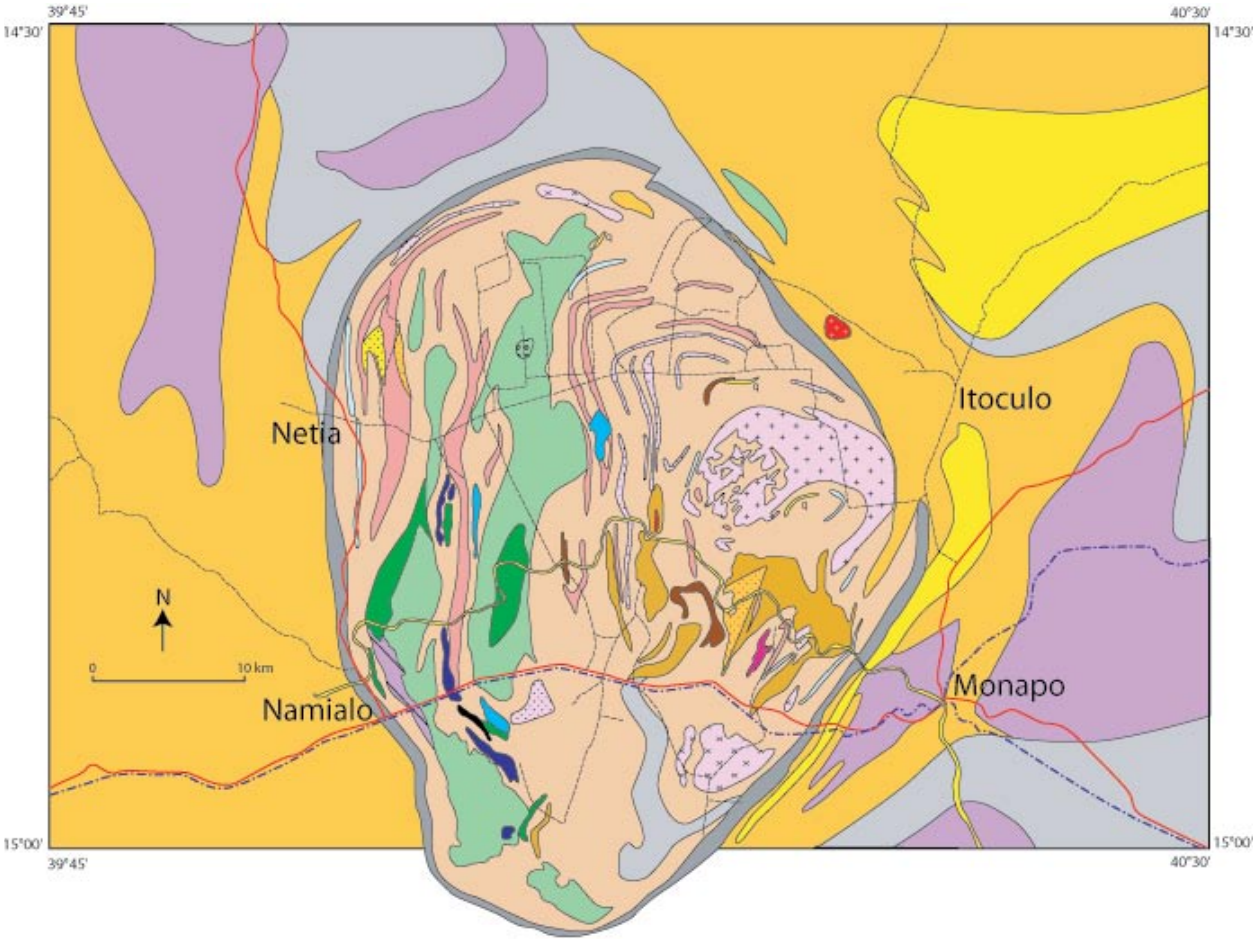

Figure 6. Regional geology of the Monapo Structure. Legend in figure 7.

the Nampula Subprovince (Macey *et al*, 2006; Fig. 6). The Metacheria Metamorphic Complex comprises rocks of upper amphibolite to granulite facies, with a strong gneissic fabric. These rocks form the basement in the Monapo Structure that the Mazerapane and Ramiane Suites have intruded into. These two younger suites are to a large extent undeformed (Macey *et al*, 2006). The Mazerapane Suite is composed of alkaline, ultramafic and mafic rocks that are mostly located in the western parts of the structure. The Ramiane Suite is composed of the alkaline, felsic counterpart to the Mazerapane Suite and is located in the eastern parts of the structure. Orthogneisses in the Monapo Structure that differ from the Metocheria Metamorphic Complex gneisses in texture, mineralogy and grade of metamorphism have been assigned to the Nampula Subprovince (Macey *et al*, 2006).

The Ramiane Suite comprises two major plutons, the Carapira and the Ramiane Plutons, with somewhat different compositions. The Carapira is a small circular outcrop of hornblende-quartz-syenite-gneiss and the Ramiane Pluton is mostly comprised of alkali granites. Samples for this study were taken from the Ramiane Pluton (Fig. 7). Parts of the Ramiane Pluton record evidence of deformation, where the outer part of the pluton is the most deformed and appears more or less mylonitic. The amount of deformation decreases towards the centre of the Ramiane Pluton with an almost unaffected centre. The prominent garnet bearing leucocratic patches that appear locally are also undeformed. Because of the higher degree of deformation on the edge of the pluton it has been suggested that the deformation is intrusion related (Macey *et al,* 2006). The pluton is

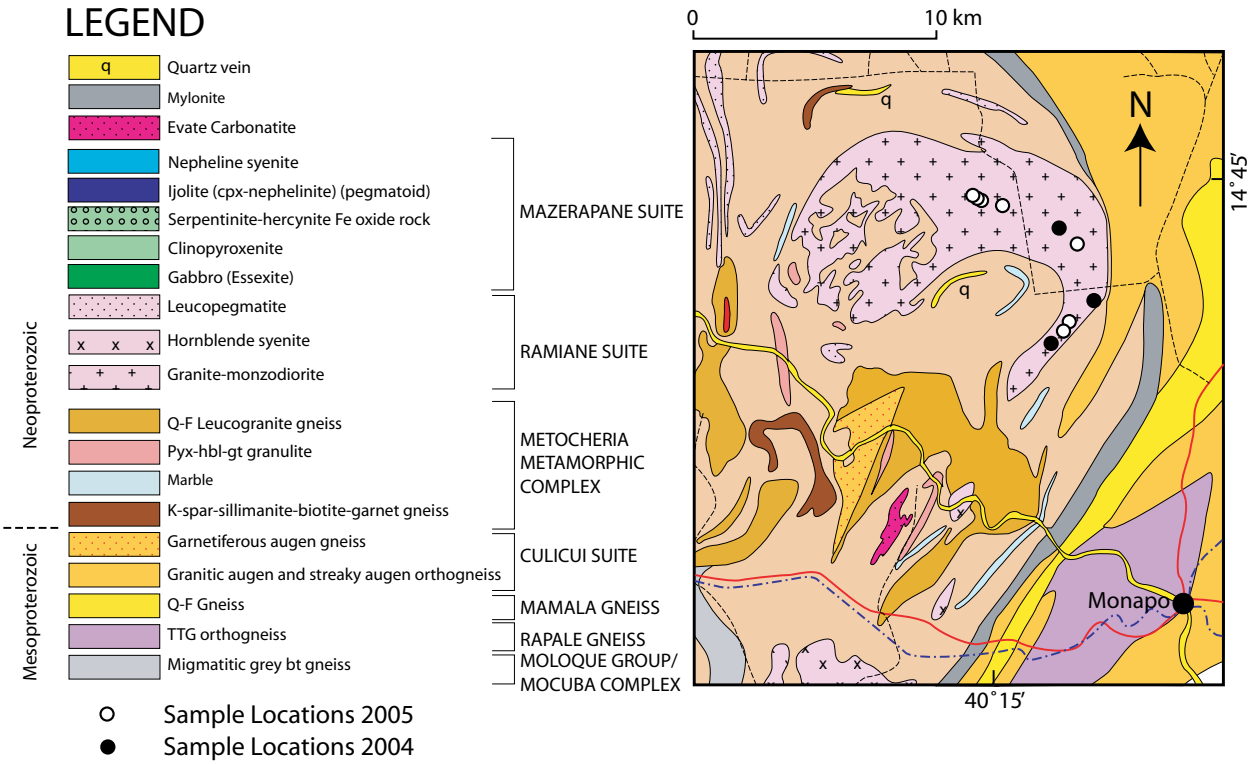

Figure 7. Close up of the geology of the Ramiane Pluton indicating the location of samples examined in this study.

encompassed by a 1-3 km broad "belt" of high radiometric signal, believed to be the result of a metasomatic alteration of the surrounding rocks by the intrusion of the Ramiane Pluton (Macey *et al*, 2006, Siegfried, 1999)

2.5.2. Structure

The structures of the Monapo Structure show different generations of deformation. This is clearly evident in, for example, the Metacheria rocks that are locally incorporated within the Ramiane Pluton as they have a linear fabric that does not exist in the Ramiane (Fig. 8). The overall trends of the rocks in the Monapo Structure vary from a clearly north-south emplacement trend as in the case of the relatively undeformed Mazerapane Suite, to a deformation trend towards north-northwest apparent in the isoclinal folding of the Metacheria basement rocks. The isoclinal folding may be correlated with the intrusive events of the Ramiane and Mazerapane Suites. The mylonite zone surrounding the Monapo Structure is evidence for a major shear event that has occurred. However, there are also several major shear zones cutting through the Monapo Structure.

The rocks within the Monapo Structure tend to follow the mylonite zone, however the further towards the centre the weaker the mylonitic overprint is. There are currently no structural measurements of the mylonite that can give hints to whether it is an anti- or synform structure. However if this could be arranged it would be of

Figure 8. Metocheria rocks within the Ramiane Pluton is evidence of their relative relationship

great importance for the history of the Monapo Structure. The linear trends within the Structure differ substantially from the surrounding Nampula Subprovince where the trends are more towards east-northeast, and this could possibly be taken for evidence for the klippe theory. The structures inside the Monapo have not been part of the major investigations within this thesis, however its importance is not underestimated. With more structural measurements the issue of whether the structure is allochthonous or not can be addressed.

2.5.3. Geochronology

The oldest rocks within the structure are slivers of the 1075 Ma, sheared tonalitic-trondhjemitic-granodioritic orthogneiss and the garnet bearing augen gneisses of the Mesoproterozoic Culicui Suite. The remaining rocks are younger and range from the Neoproterozoic to recent. The Neoproterozoic Metacheria Metamorphic Complex can be divided into two groups; the sedimentary derived rocks and the igneous derived rocks. The data from the SHRIMP suggest an intrusive age of 634 ± 8 Ma and a metamorphic event at 579 ± 11 Ma. The Neoproterozoic Ramiane and Mazerapane Suites have intruded into the Metacheria basement and SHRIMP data for the Ramiane will be discussed later in this thesis. The younger Evate Carbonatite, as well as intrusive granites and quartz veins make up the Pan-African Murrupula Suite. The youngest geological deposits are the recent alluvial sediments along the perennial Monapo River.

3. PETROLOGY AND MINERAL CHEMISTRY

3.1. Petrology

The Ramiane Pluton is a fairly homogenous felsic pluton. The average grain size is relatively coarse and is quite uniform throughout the rock with a few exceptions of areas of finer grain size, and some with a more pegmatitic appearance (Fig. 9A and B). The evidence for a metamorphic overprint in the rock takes the shape of a subtle gneissocity showing in parts of the pluton (Fig. 9C). The most evident area of heterogeneity is the leucocratic garnet-bearing patches (Fig. 9D, E and F). These patches are clearly different from the rest of the host rock due to the garnet and the halos of quartzo-feldspatic material that surrounds them. The garnet in the pluton is mostly apparent in these patches, but can also be found as part of the more homogenous host rock

The mineral assemblage in the Ramiane Pluton is dominated by feldspars, quartz, garnet, amphiboles, micas, and oxides with minor apatite and zircon present. Both K-feldspar and plagioclase are present with an average grain size of 2-4 mm in diameter. However there are larger grains, ~6 mm, randomly distributed in the rock. The plagioclase is often albite twinned. Alteration from feldspar to mica is evident from the sericitisation of the feldspar grains. Many of the microcline grains display an obvious tartan twinning texture, and blebs of plagioclase composition are a common feature within these grains. This texture is referred to as perthite and in this pluton the perthitic textures do not always cover the whole K-feldspar grain, but is somewhat restricted to the central parts with a rim of non-perthitic K-feldspar towards the margin of the grains. The plagioclase has a typical myrmekitic texture in some of the smaller, 0.2-0.5 mm, grains. The quartz grains are 0.2-3 mm in diameter, but similar to the feldspars, larger grains also occur randomly dispersed in the rock. Most of the quartz grains show undulose extinction. The quartz occasionally show needle shaped inclusions of what appear to be rutile, as

well as abundant fluid inclusions.

Different pleochroic colours in the amphiboles indicate that there are at least two compositions of amphibole, one with khaki-green to green-brown pleochroism and the other with a more blue to green pleochroism. The grains differ from 0.2 to 4 mm in diameter, and are anhedral to euhedral in shape. The larger more euhedral amphiboles are the khaki green ones and they also show more of a typical amphibole cleavage (124° / 56°) than the others. However there are traces of it in all the different amphibole minerals (Fig. 10A). In some parts of the rocks there are "spongy" textures involving mainly

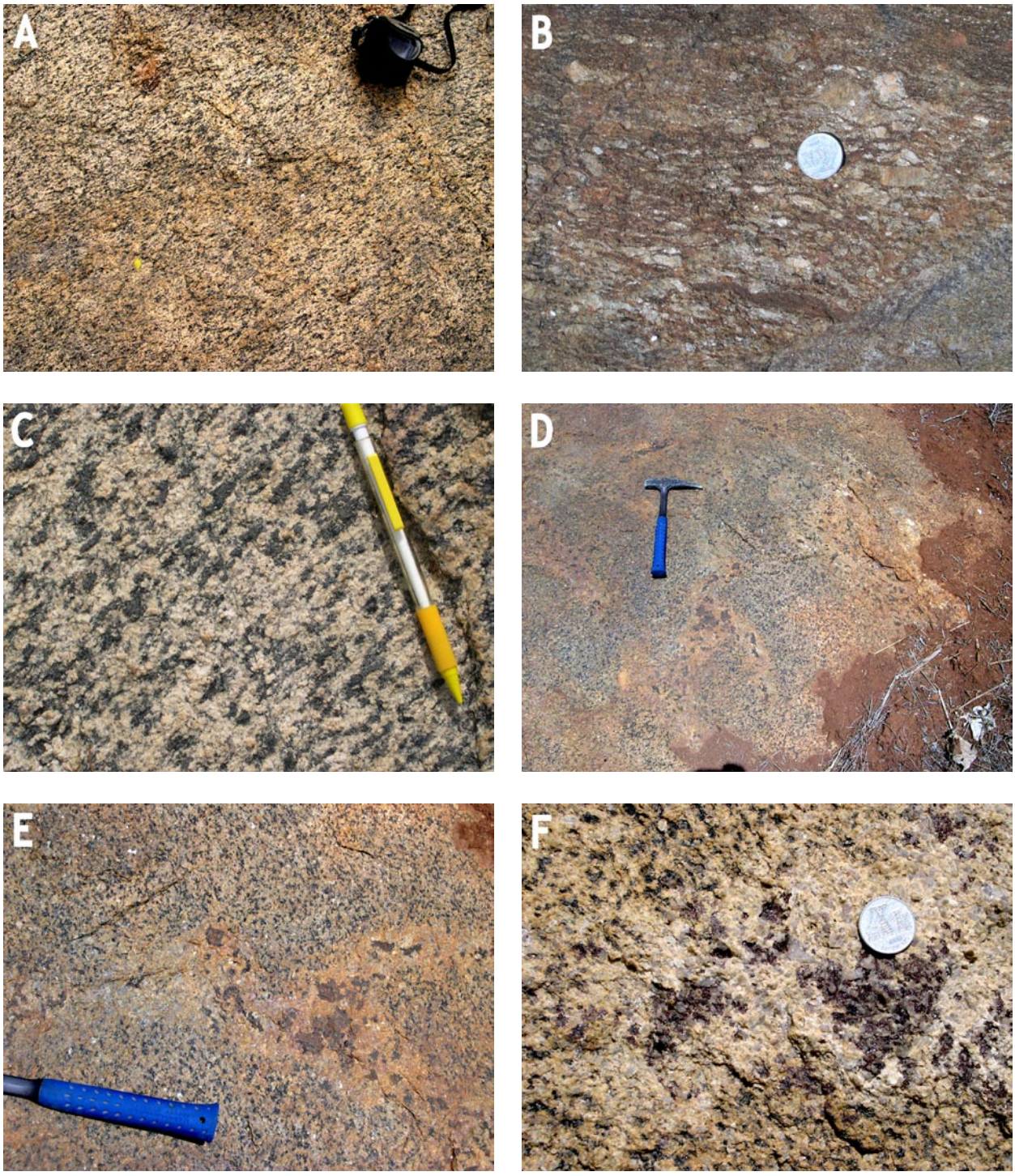

Figure 9 A) a typical, relatively coarse grained area of the pluton. B) a more pegmatitic locality with larger feldspar grains. C) a subtle gneissocity showing to a large extent in the rock. D and E) larger scale leucocratic patches with coexisting garnet. F) a smaller patch of leucocratic minerals surrounding garnet.

amphiboles, oxides, plagioclase, K-feldspar and quartz. In general, the locations with the spongy textures have more fine grained minerals than the rock as a whole (Fig. 10B). The finer grained samples of the Ramiane Pluton have much smaller amphibole grains than the other parts of the rock, and here they are largely altered to what appears to be oxides (Fig. 10C).

The garnets in the rock are large anhedral to slightly subhedral grains, with a diameter of between 2 and 10 mm. They are typically surrounded by feldspars and quartz, but

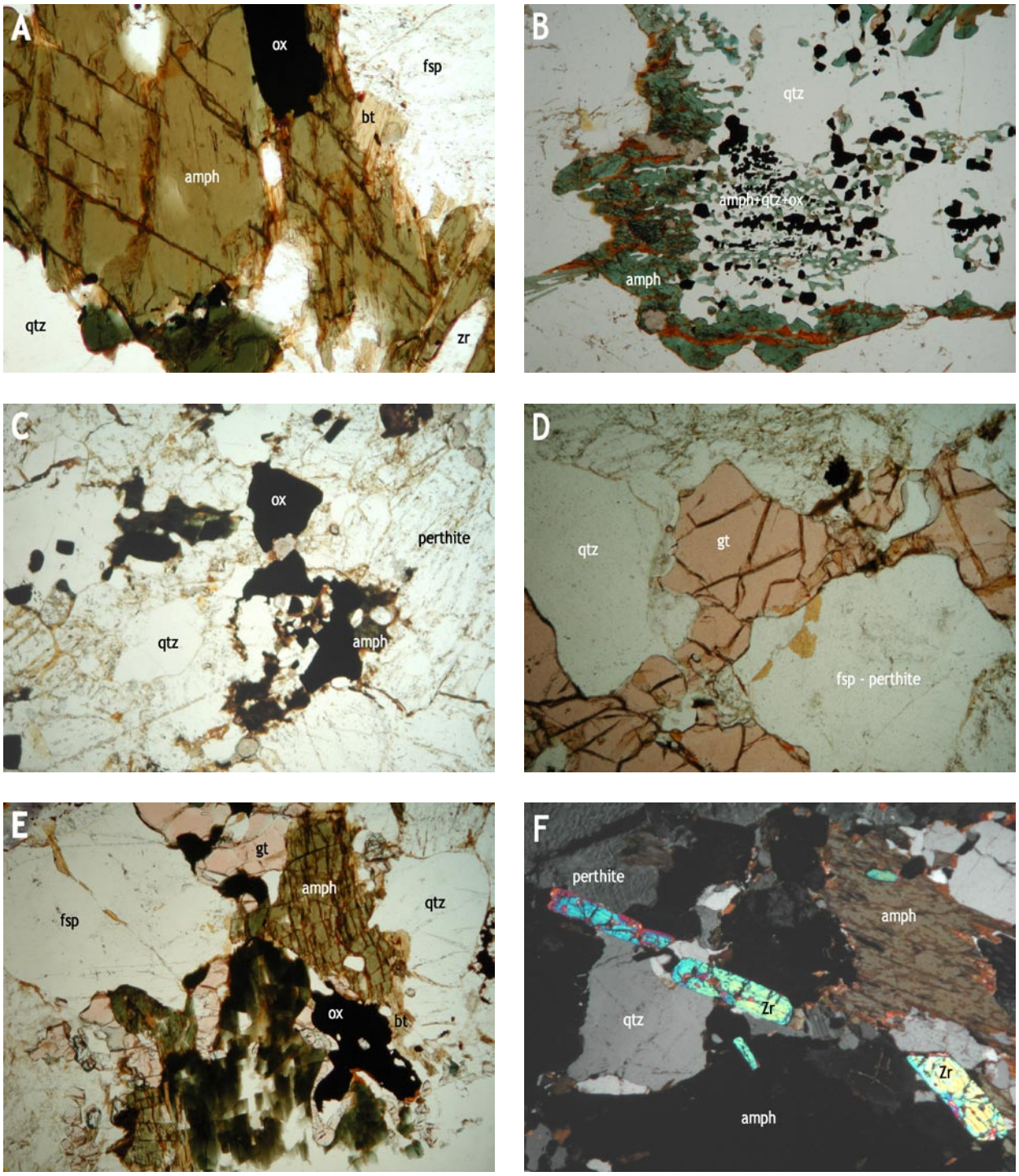

Figure 10. A) coexisting amphibole and biotite with the amphibole showing typical amphibole cleavage. Field of view ~2 mm. B) spongy amphibole breakdown area. Field of view ~2 mm. C) small and altered amphibole in the finer grained host rock. Field of view ~3 mm. D) garnet typically surrounded by leucocratic minerals. Field of view ~3 mm. E) area where garnet coexists with biotite and amphibole. Field of view ~3 mm. F) larger, euhedral grains of unzoned zircons Field of view ~3 mm.

amphiboles and biotite are also found in the vicinity (Fig. 10D, E and 11A). There does not seem to be an obvious zoning of the grains but smaller variations in composition from different parts of the rock exist. Micas are minor minerals in the rock, with biotite more abundant than muscovite. The white mica is almost exclusively associated with the sericitisation of the feldspar. The biotite grains are tabular in shape and 0.2-1.5 mm in diameter. It is commonly found intergrown with the amphibole, but they also appear to be break down products of the same

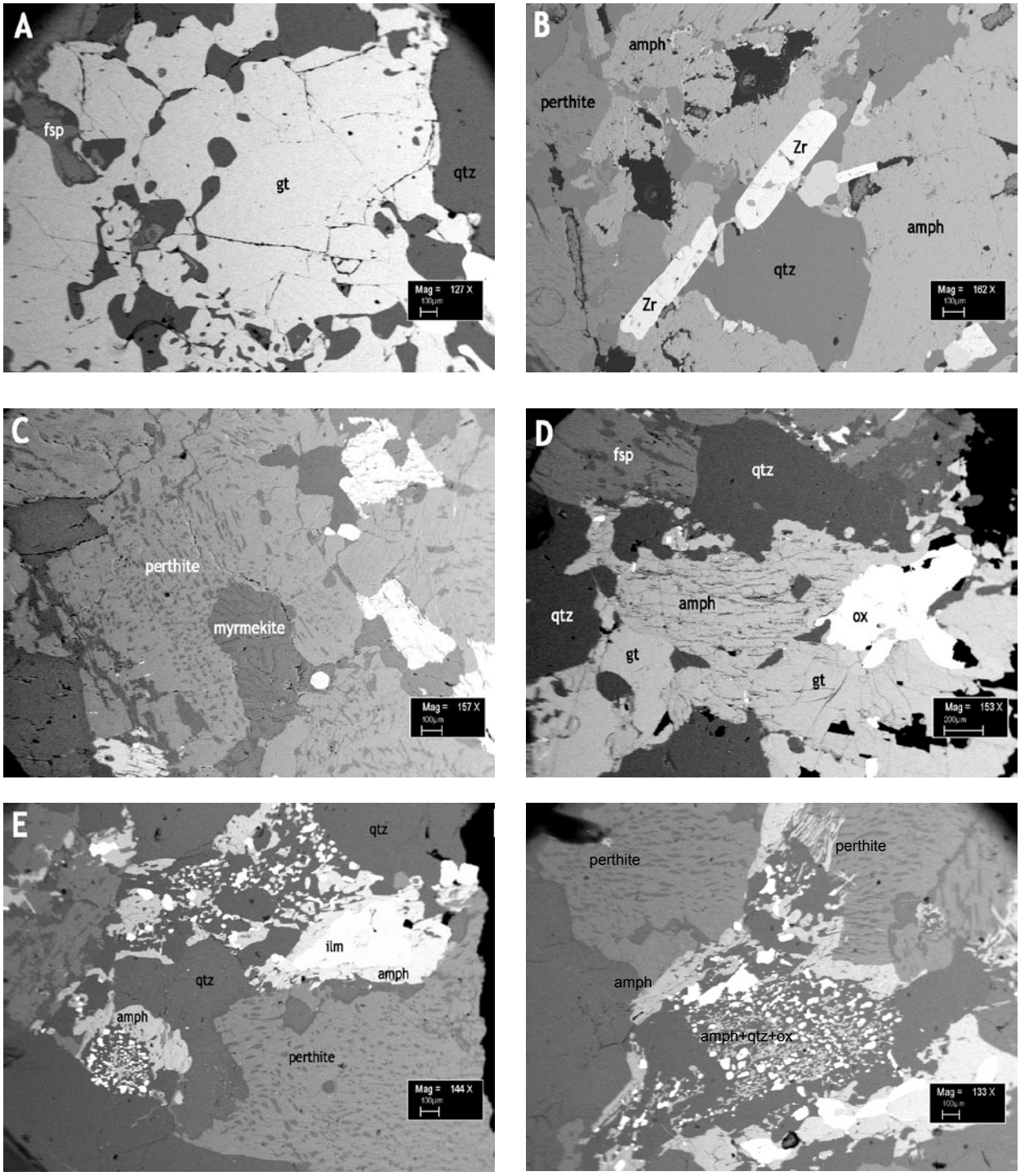

Figure 11. A) garnet surrounded by leucocratic minerals. Field of view ~3.0 mm. B) occasionally appearing larger zircon grains. Field of view ~2.5 mm. C) perthitic and myrmekitic textures in feldspars. Field of view ~2.5 mm. D) typical appearance of hastingsite, here coexisting with garnet. Field of view ~2.5 mm. E) spongy amphibole breakdown textures with coexisting ilmenite. Field of view ~2.8 mm. F) a more blocky area of amphibole breakdown creating the spongy texture evident in the photo. Field of view ~3.0 mm.

in certain areas. This can be observed mainly at the margin of the amphiboles. The oxides in the rock are mainly ilmenite, magnetite and/or hematite. The grains are up to 1 mm in diameter. Zircon and apatite are 0.1-0.3 mm diameter in size, with a small group of larger euhedral zircon grains with lengths of approximately 0.7 mm (Fig. 10F and 11B). The zircon is occasionally zoned and varies in shape from almost tabular to elliptical. The apatite is commonly rice shaped, and appears to be coated by allanite.

3.2. Mineral Chemistry

3.2.1. Feldspars

The end member composition of the K-feldspar does not vary very much, with Or_{89-95} and Ab_{5-11}. Barium occasionally substitutes for potassium in the K-feldspars. The plagioclase generally varies from An_{13-24}, Ab_{74-85} and Or_{0-4}.

Perthite is a common texture in the feldspar grains and show small blebs of plagioclase in the K- feldspar grain (Fig. 11C).

Representative mineral data for feldspars as well as biotite, amphibole and garnet is shown in Table 1.

3.2.2. Garnet

The site allocation of the major cations in garnet indicates that the garnet is almandine-andradite in composition, with an almandine variation X_{Alm} between 0.69 and 0.77, and an andradite variation X_{And} between 0.13 and 0.18. Between these two garnet components there is a weak negative correlation. The amount of pyrope in the garnet is low with X_{Py} between 0.00 and 0.04. This mirrors the relatively low Mg content in the rock as a whole. The spessartine and grossular contents are both low with X_{Sp} between 0.03 and 0.10, and X_{Gro} in the range of 0.0-0.08. The compositional variations described above do not appear to be related to the textural environment in which the garnet

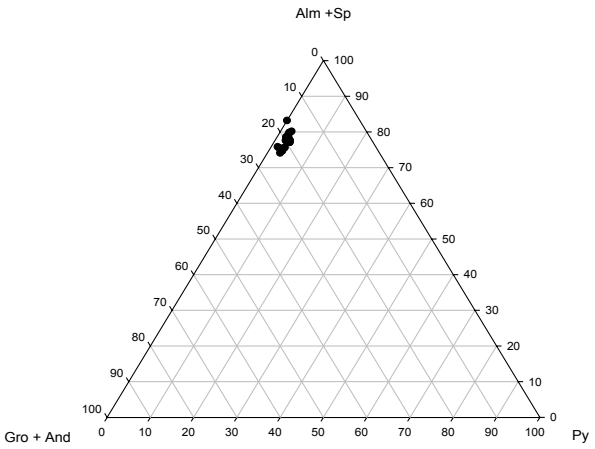

Figure 12. Compositional variation of the garnet in the Ramiane Pluton.

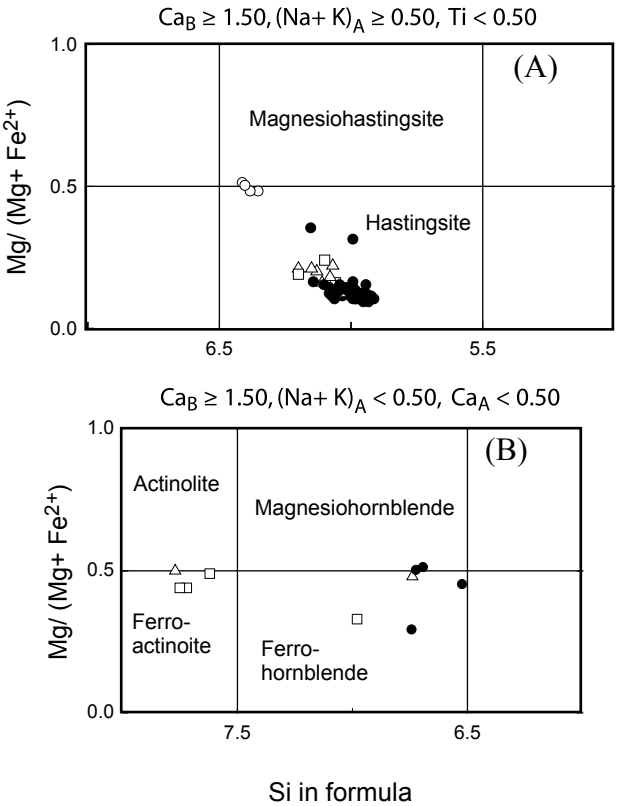

Figure 13. Amphibole classification diagram reworked after Leake et al, 1997. A, White circles represent amphibole from finer grained host rock. The most common amphibole in the host rock is the hastingsite, black symbols. The breakdown products from the spongy areas are the slightly enriched silica amphibole represented by the white triangles and squares; B, More locally occurring silica rich amphiboles.

Sample no.	17X					20					15X				23			
Mineral	Amph	Bt	Ksp	Plag	Gt	Amph	Bt	Ksp	Plag	Gt	Amph	Amph	Bt	Fsp	Amph	Amph	Bt	
SiO2	36.85	35.87	65.51	63.98	36.06	37.39	35.13	65.11	64.20	35.32	42.98	37.53	34.40	65.72	44.79	51.17	33.93	
TiO2	1.81	3.34	0.00	0.00	0.00	1.17	3.66	0.00	0.00	0.00	0.59	1.07	4.87	0.00	1.08	0.07	4.20	
Al2O3	10.68	13.61	18.38	23.76	18.78	10.49	11.92	18.19	21.57	19.01	6.09	10.10	12.52	18.48	7.58	1.41	14.95	
Fe2O3	8.47	0.00	0.00	0.00	5.27	9.70	0.00	0.00	0.00	5.81	8.70	8.71	0.00	0.00	7.72	1.64	0.00	
FeO	24.43	30.89	0.00	0.00	31.49	24.17	31.77	0.00	0.00	31.78	20.92	24.72	32.25	0.00	15.30	21.18	30.05	
MnO	0.45	0.00	0.00	0.00	2.11	0.45	0.00	0.00	0.00	2.03	1.20	0.62	0.00	0.00	0.65	0.26	0.08	
MgO	1.64	4.03	0.00	0.00	0.67	1.78	3.61	0.00	0.00	0.48	4.87	2.00	3.41	0.00	8.69	9.51	4.01	
CaO	10.20	0.00	0.00	4.01	6.48	10.49	0.00	0.00	3.36	5.89	10.86	10.95	0.00	0.00	10.90	12.41	0.00	
Na2O	1.77	0.00	0.61	9.04	0.00	1.64	0.00	1.09	9.38	0.00	1.16	1.65	0.00	1.07	1.43	0.29	0.23	
K2O	2.40	9.63	16.38	0.55	0.00	2.38	9.27	15.80	0.00	0.00	1.15	2.17	9.51	15.66	0.97	0.13	9.33	
BaO	0.00	0.00	0.52	0.00	0.00	0.00	0.00	0.00	0.00	0.00	0.00	0.00	0.00	0.00	0.00	0.00	0.00	
Total	98.70	97.36	101.41	101.35	100.86	99.65	95.36	100.19	98.50	100.32	98.52	99.53	96.97	100.92	99.12	98.06	96.78	
Cation total																		
No. of O	23	22	32	32	12	23	22	32	32	12	23	23	22	32	23	23	22	
Si	5.95	5.83	11.97	11.17	2.94	6.06	5.87	11.97	11.53	2.90	6.98	5.95	5.67	12.00	6.72	7.72	5.53	
Al	1.95	2.60	3.96	4.89	1.80	1.95	2.35	3.94	4.56	1.84	0.87	1.90	2.44	3.98	1.34	0.25	2.87	
Ti	0.17	0.41	0.00	0.00	0.00	0.14	0.46	0.00	0.00	0.00	0.00	0.26	0.60	0.00	0.12	0.01	0.51	
Fe	4.58	4.19	0.00	0.00	2.47	4.28	4.44	0.00	0.00	2.54	3.65	4.36	4.45	0.00	2.79	2.86	4.09	
Mg	0.35	0.97	0.00	0.00	0.08	0.48	0.90	0.00	0.00	0.06	1.32	0.44	0.84	0.00	1.94	2.14	0.97	
Mn	0.00	0.00	0.00	0.00	0.15	0.09	0.00	0.00	0.00	0.14	0.17	0.08	0.00	0.00	0.08	0.03	0.01	
Ca	1.88	0.00	0.00	0.75	0.57	1.89	0.00	0.00	0.65	0.52	1.85	1.91	0.00	0.00	1.79	2.01	0.00	
Na	0.52	0.00	0.22	3.06	0.00	0.49	0.00	0.39	3.26	0.00	0.38	0.58	0.00	0.38	0.42	0.08	0.07	
K	0.47	1.99	3.82	0.12	0.00	0.36	1.98	3.70	0.00	0.00	0.21	0.44	2.00	3.65	0.19	0.03	1.94	

Table 1. Representative mineral chemistry data from different parts of the Ramiane Pluton. Sample JM05MC-17X and JM05MC-20 are garnet bearing.

occurs and there is no obvious compositional zonation in the garnets (Fig. 12).

3.2.3. Amphibole

There are several different types of amphibole in the Ramiane Pluton (Fig. 13). Amphiboles associated with the spongy textures demonstrate a gradual change in composition from a relatively high K, Al and Na content, to a more Si, Mg and Mn rich version. Recalculation of the amphibole compositions according to Leake et al. (1997) indicates that this compositional variation reflects a change from a lower Mg# hastingsite composition (Fig. 11D), to a higher Mg# hastingsite composition as well as a ferro-hornblende composition for those amphiboles where the total Na+ K cations on the A-site is less than 0.50 (Fig. 11E and F). Amphibole in the finer grained samples has a higher Mg#, 40-50, compared to the coarse grained areas where the Mg# is closer to 10-15 in most cases. Most of the amphiboles with the higher Mg# are hastingsite. However, there are a few bordering on the magnesio-hastingsite field. There are also amphiboles with higher Si content locally in the host rock. These are not connected with the spongy textures mentioned above. These amphiboles are ferro-actinolite, and ferro- and magnesio-hornblendes. These amphiboles have their A-sites filled up to less than 50%, with the A-site of the ferro-actinolites approximately 90% vacant (nomenclature from Leake et al, 1997). The Na cation total ranges from 0.47 to 0.58 in the most common amphibole, hastingsite. In the fine grained sample JM05MC-21 the Na cation total is slightly lower with values very close to 0.40. However this is still hastingsite. The ferro-actinolites have Na totals below 0.1.

3.2.4. Biotite

The biotite in the pluton is fairly homogenous with minor variations in composition. It is rich in Fe and Ti. The Ti cation average is 0.43, and the distribution of the Ti in the biotite is very homogenous and there are only a few values that differ from the others. The Fe cation average is 4.24, and in the Fe there is also a fairly homogenous trend. However there is a wider range from 3.93 to 4.63. The Ti and the Fe fill up almost 80% of the M-site in the biotite, with Mg filling up the most of the remaining positions (15%). Due to the high Ti and Fe the Mg# is relatively low and varies between 12 and 21, with an average of 17. Both the Na and the Mn have very low cation totals. The Mn varies and forms two distinct groups. The first group has no Mn cations and the second group has 0.05-0.1. The Na shows a larger variation in cation total in the biotite and has an average of 0.86.

4. GEOCHEMISTRY AND STABLE ISOTOPES

4.1. Whole rock geochemistry

4.1.1. Major elements

Samples examined in this study have been classified as granitic in composition with one exception, the more mafic sample JM05MC-15, that is syenodioritic in composition. The alkaline granites mentioned above are in some cases transitional in composition towards granodiorite or subalkaline granite (Fig.14).

The major element analyses discussed in this chapter are presented in Fig. 15, as well as in Table 2. and are based on hydrous element wt%. The samples are very homogeneous, and most binary diagrams have a slight negative trend. The SiO_2 content varies over a small range from 63-70 wt%. The relatively low and consistent Al_2O_3 content of the samples, between 12-14 wt%, produces a marked horizontal trend when plotted against wt% SiO_2. The TiO_2 content varies very little from 0.4 to 1.0 wt%. The total

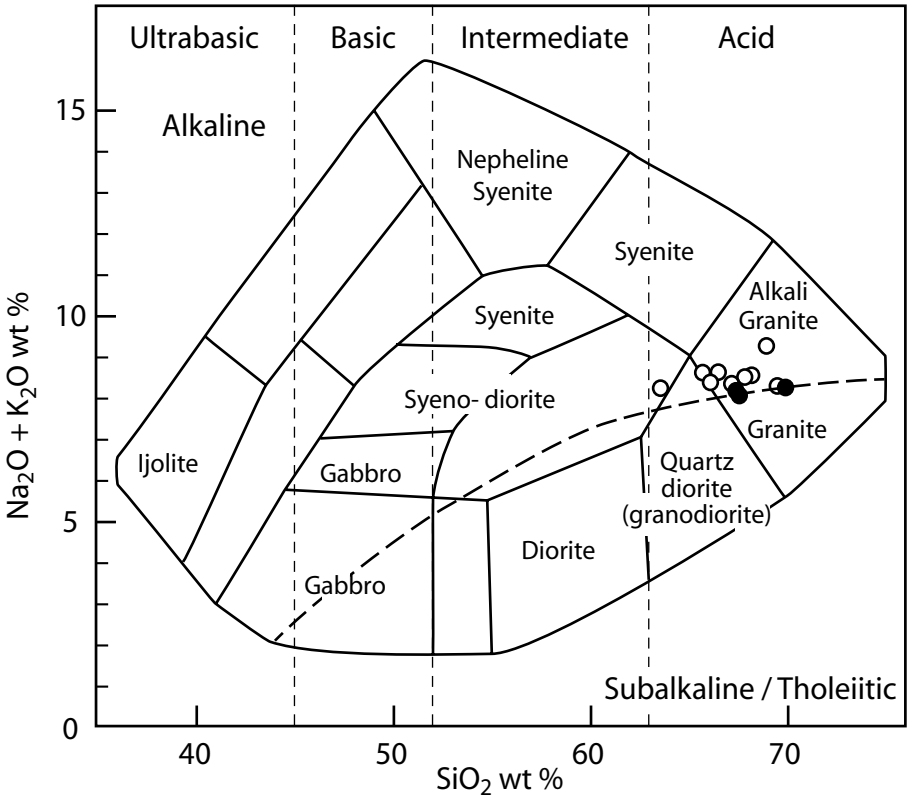

Figure 14. Classification diagram and nomenclature of plutonic rock types using a TAS diagram by Cox et al, (1979) adapted by Wilson, (1989). Dotted line separates subalkaline rocks from alkaline rocks. All elements in anhydrous wt%. White circles represent samples analysed 2006 in Stellenbosch, and black circles represent samples analysed 2005 at a different location.

iron, Fe_2O_3, shows the largest variation, except from SiO_2, with between 5 and 10 wt%. MnO contents are low and range from 0.05-0.15 wt%. Noticeable here is sample JM05MC-19, which is a sample of one of the garnet bearing, leucocratic patches. Except for sample JM05MC-15, which is not garnet bearing, sample JM05MC-19 has the highest MnO wt%. The MgO contents are relatively low and range from 0.2-1 wt%. CaO and the Na_2O contents show quite similar trends with between 1.5-3, and 2.5-3.5 wt% respectively. Wt% K_2O ranges from 4.5-5.5 wt%. In this case, increasing K_2O is coupled to increasing SiO_2.

4.1.2. Trace elements

The Zr values from the pluton stand out as high compared to Zr values from surrounding rocks from the Nampula Subprovince and within the Monapo Structure. Zr values range from 585 ppm to 1003 ppm, with most values between 700-800 ppm. Ba contents are also relatively high, with variations between 711 and 1815 ppm although most values are above 1000 ppm. The Th, which shows a clear peak in the multi element diagram, ranges between 11 and 51 ppm, and the Pb between 31 and 55 ppm. The highest values for both the Th and the Pb are in sample JM05MC-15. This is the sample where the large zircons occur (Fig. 10F). Compared to surrounding rocks of both Nampula Subprovince and Monapo origin the Nb values are higher, but not unusually high. The Rb also shows higher values than the surrounding rocks and the Sr lower values. This could suggest a different evolution of the pluton compared to the surrounding rocks. By using a discrimination diagram plotting Y vs Nb (after Pearce *et al*, 1984) and a Zr vs Ga/ Al, A-type discrimination diagram (after Whalen *et al*, 1987a) the tectonic setting is suggested as "Within Plate" and the rock type as an A-type granite (Fig. 16). In general the trace element plots are very scattered, with a few exceptions that indicate trends. These trends are almost exclusively negative. The Zr vs Nb diagram does not clearly give a uniform result which can be due to a slight compatibility difference

Sample No.	JM05MC 15	JM05MC 18	JM05MC 19	JM05MC 19B	JM05MC 20	JM05MC 21	JM05MC 22	JM05MC 23	JM05MC 24	JM05MC 25
XRF Majors wt % oxide										
SiO_2	62.89	64.50	65.24	63.88	66.76	64.45	67.27	65.05	65.91	65.26
TiO_2	0.94	0.62	0.65	0.67	0.58	0.83	0.56	0.68	0.54	0.57
Al_2O_3	13.26	13.63	13.69	13.48	13.51	13.65	12.05	12.25	12.35	12.93
Fe_2O_3	9.46	6.48	7.25	7.24	6.15	6.33	6.09	6.75	5.54	5.60
MnO	0.14	0.10	0.15	0.11	0.11	0.10	0.10	0.10	0.10	0.09
MgO	0.95	0.61	0.84	0.71	0.60	0.81	0.37	0.59	0.64	0.70
CaO	2.96	2.21	2.59	2.62	2.13	2.19	1.86	2.76	1.47	2.09
Na_2O	3.37	3.26	3.22	3.28	3.35	3.09	2.76	3.33	3.59	3.46
K_2O	4.70	5.05	4.96	5.04	5.03	5.15	5.23	4.73	5.22	4.69
P_2O_5	0.26	0.17	0.17	0.18	0.15	0.22	0.11	0.19	0.15	0.17
LOI	1.96	1.96	2.43	2.54	2.07	3.04	2.96	3.32	2.50	3.00
TOTAL	100.91	98.60	101.19	99.73	100.43	99.86	99.36	99.74	98.00	98.56
SiO2*	63.56	66.48	66.06	65.72	67.87	66.19	69.57	67.24	68.98	68.28
XRF Traces ppm										
V	6	5	6	0	0	12	0	0	3	1
Cr	12	13	11	13	10	26	31	28	8	13
Co	127	167	175	150	163	157	163	202	192	210
Ni	23	12	16	17	17	28	24	19	13	11
Cu	17	16	16	16	15	14	12	14	16	15
Ga	26	27	25	26	27	22	24	27	29	29
Rb	145	225	185	195	222	131	169	143	168	253
Sr	168	127	128	132	125	178	85	134	141	117
Y	97	94	136	101	90	76	65	75	102	96
Zr	855	764	791	857	696	884	793	894	655	651
Nb	37	30	32	31	28	41	35	45	22	24
Ba	1484	1228	1290	1322	1233	1319	755	1343	1815	910
Pb	55	44	41	41	45	35	31	36	38	41
Th	51	47	41	51	38	21	15	27	40	49
U	1	0	4	0	0	5	9	7	0	3
Rb/ Sr	0.86	1.77	1.45	1.48	1.78	0.74	1.99	1.07	1.19	2.16
ASI	0.66	0.74	0.71	0.69	0.74	0.74	0.71	0.63	0.72	0.72
LA ICP- MS REE ppm										
La	962.4	428.1	671.1	284.16	558.6	557.4	615.3	625.5	498.6	—
Ce	240.96	231.06	223.92	170.94	206.01	116.76	132.72	148.2	115.86	—
Pr	31.05	29.07	29	18.28	26.55	17.61	17.9	19.79	16.93	—
Nd	162.93	151.2	151.65	95.13	136.98	91.71	95.79	102.51	85.02	—
Sm	29.64	27.44	28.32	17.15	24.25	20.26	17.84	19.43	16.66	—
Eu	4.45	3.43	3.48	2.14	3.14	2.82	2.88	3.34	3.54	—
Gd	9.19	25.21	26.87	15.39	21.85	19.44	16.25	16.72	16.12	—
Tb	3.98	3.6	4.23	2.42	3.33	2.71	2.35	2.42	2.39	—
Dy	28.25	26.15	33.36	16.04	22.51	18.11	15.06	16.42	16.76	—
Ho	5.11	4.61	6.59	2.97	4.17	3.52	2.94	3.12	3.2	—
Er	14	12.47	21.4	7.48	11.23	8.64	7.25	7.87	8.34	—
Tm	2.13	1.89	3.5	1.18	1.72	1.33	1.21	1.6	1.28	—
Yb	13.7	12.04	25.89	6.78	10.44	7.64	7.14	7.35	7.24	—
Lu	2.06	1.68	3.93	1.02	1.57	1.16	1.12	1.12	1.08	—
REE_{tot}	1510	958	1233	641	1032	869	936	976	793	
Eu/ Eu*	0.82	0.4	0.39	0.4	0.42	0.43	0.52	0.57	0.66	
Stable Isotope Ratios ‰										
$\delta^{18}O_{WR}$	10.0	9.8	10.3	9.9	10.4	10.3	10.3	10.1	10.1	10.7
$\delta^{18}O_{Qtz}$	11.4	11.7	11.4	11.2	11.6	11.5	—	12.2	11.9	—

Note: SiO_2*= Anhydrous SiO_2, LOI= Loss Of Ignition, ASI= Aluminium Saturation Index (from Debon et al, 1983), WR= Whole Rock

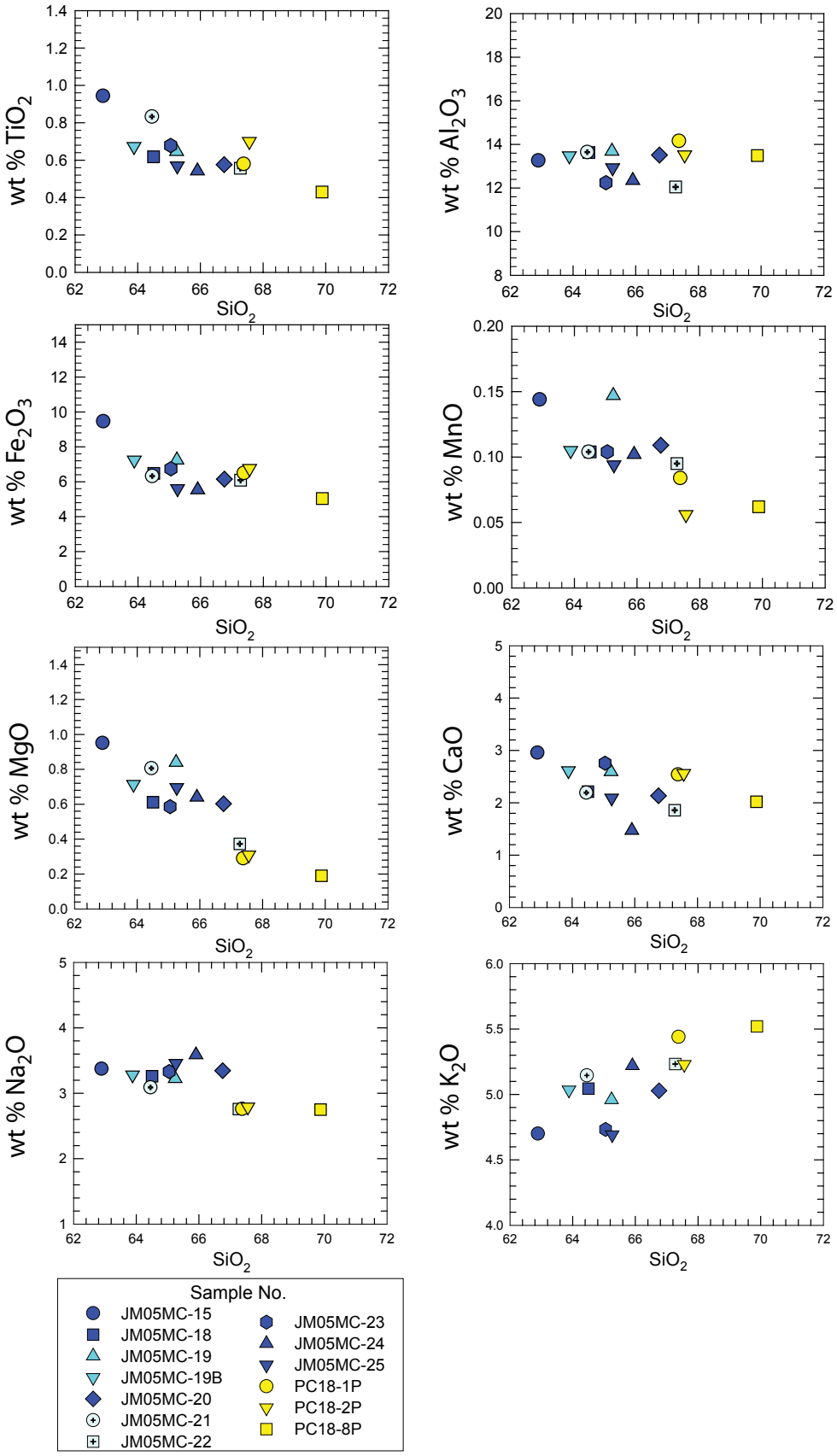

Figure 15. Major element Harker diagrams from JM05MC15- JM05MC25 (white circles in other diagrams) and PC18-1P,PC18-2P, PC18-8P (black circles in other diagrams). All elements in anhydrous wt%.

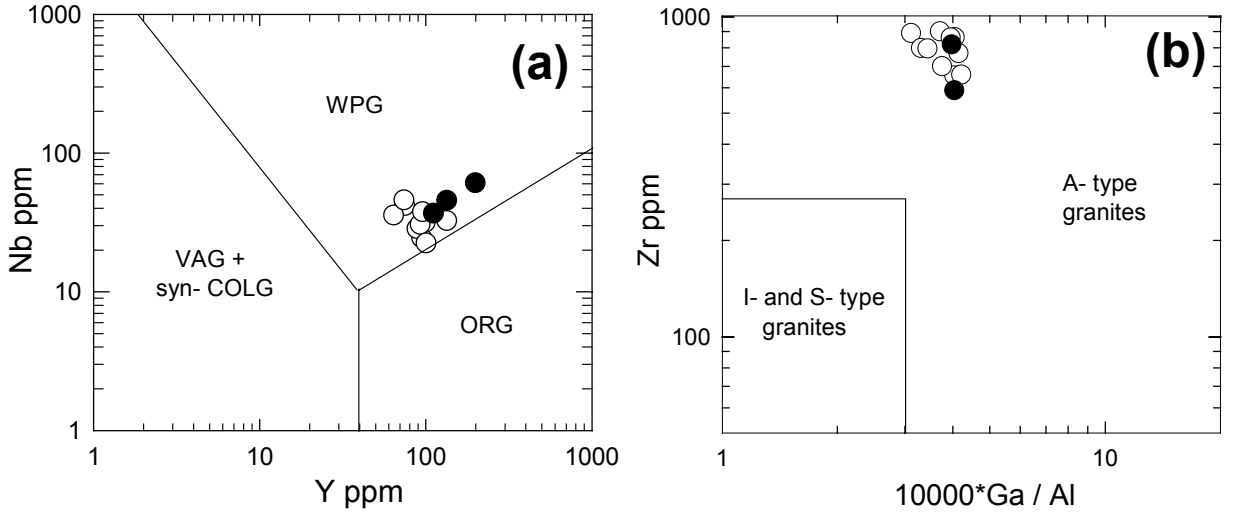

Figure 16. A) Y vs Nb discrimination diagram for granites after Pearce et al. (1984). Fields for WPG= Within Plate Granites, ORG= Ocean Ridge Granites, VAG= Volcanic Arc Granites and syn- COLG= syn-Collisional Granites. B) Discrimination diagram for A-type granites after Whalen et al. (1987) showing A-, S-, and I- type granite fields. White circles represent samples analysed 2006 in Stellenbosch, and black circles represent samples analysed 2005 at a different location.

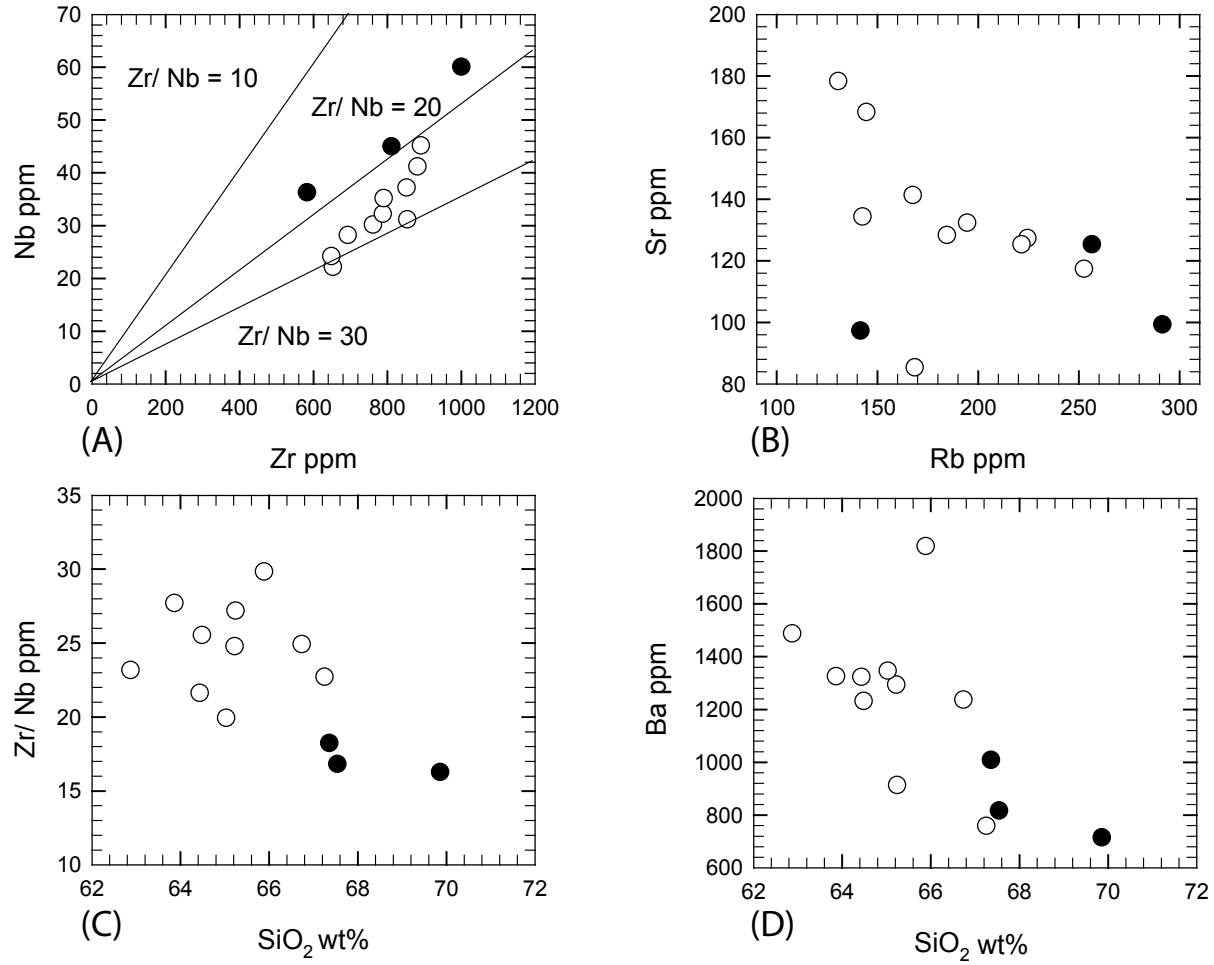

Figure17. A) Nb vs Zr diagram showing the ratio between the two elements. Compatibility difference can be the reason for the deviation from a unanimous trend line. B) Rb vs Sr diagram showing a typical negative trend due to compatibility differences. C) Diagram of SiO_2 vs Zr/ Nb showing a typical, for these data, scattered plot. The lack of trend can be a reflection of the original protolith conditions. D) Diagram of SiO_2 vs Ba showing a negative trend that possibly could indicate K-feldspar in the protolith. White circles represent samples analysed 2006 in Stellenbosch, and black circles represent samples analysed 2005 at a different location. Values based on anhydrous element wt %.

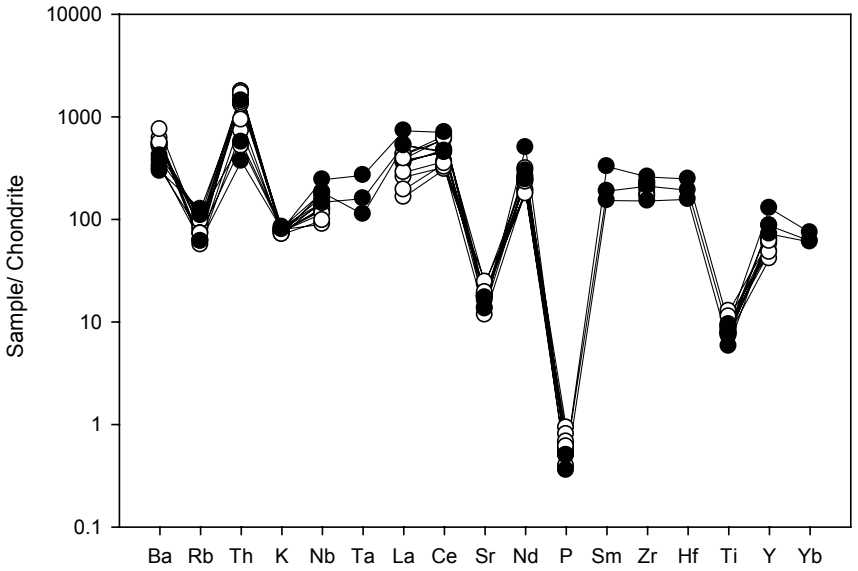

Figure 18. Multi element diagram reworked after Rollinson (1993). Elements in ppm and normalized to chondrite values of Sun and McDonough (1989). Overall negative trend towards the less mobile HREE. Evident peak at Th, and evident troughs at Sr, P and Ti. Samples from 2006 have less trace element analyses. White circles represent samples analysed 2006 in Stellenbosch, and black circles represent samples analysed 2005 at a different location.

between these two elements caused by different ionic charge. However, the ratios line up closest between Zr/ Nb = 20 and 30 (Fig 17A). The Rb vs Sr diagram shows the difference in compatibility between the two elements and the clear negative trend is a product of this (Fig 17B). The Zr/ Nb vs SiO_2 diagram shows a typical scattered plot with no clear trend (Fig. 17C). The scattered plots from the Ramiane Pluton could possibly reflect the original relationship between the elements in the protolith. The implications of the scattered plots of the rock analyses will be discussed later. The negative trend in the Ba vs SiO_2 diagram is possibly due to presence of K-feldspar in the protolith which is quite common for the closely related syeno-granitic rocks (Fig. 17D). It would appear possible that the K-feldspar theory is applicable here as well, as Ba can replace K in K-feldspar (Deer, Howie and Zussman, 1992).

The trace elements have been plotted on a multi-element diagram (Fig. 18), that not only uses the actual trace elements but also elements such as K. Aligning the minerals from left to right with increasing compatibility will highlight a possible contrast between the different groups in a diagram. The diagram shows positive Th and Ba anomalies and negative anomalies for Sr, P and Ti. Overall there is a slight slope with a negative trend towards the less mobile elements. The positive Ba anomaly could be connected to the fact that Ba, as mentioned above, substitutes for K in the K-feldspar. The Th anomaly could be due to a high concentration of Th in zircon or to the Pb content in the rock. However, this needs further investigation. The negative anomalies for the Sr, P and Ti can be partly related to the original composition of the protolith. If the protolith was depleted in these elements then the result will be negative anomalies in the Ramiane Pluton, especially considering that these are relatively compatible elements.

4.1.3. Rare earth elements

The total REE content of the samples analysed during 2006, averages 994 ppm, but shows a substantial range from 641 ppm to 1510 ppm. The low value of 641 ppm is from the relatively garnet free sample JM05MC-19B, and would thus reflect the known fact that garnet is a mineral with large HREE (heavy rare earth elements) storage capacity. The high value of 1510 ppm is from the more mafic, syenodioritic sample JM05MC-15. Figure 19 shows a rare earth element diagram normalised to the chondritic values of Sun and McDonough (1989). The overall trend of the diagram is

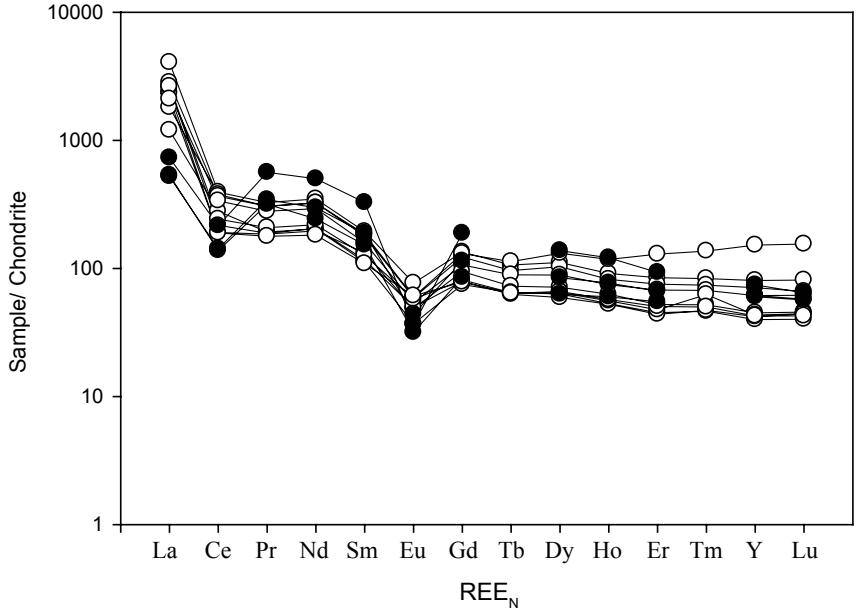

Figure 19. REE diagram. The rare earth elements have been normalized against chondrite values of Sun and McDonough (1989). Samples from 2006, white circles, have more REE analyses than the samples from 2005, black circles. The La is unusually high, possibly due to La contamination of the flux for the fuse beads. There is a clear Ce depletion and Eu anomaly in the diagram. Most samples show overall negative trend towards the HREE, but sample JM05MC-19 that shows a positive trend. This is the sample that represents the garnetiferous leucocratic patches, and not the whole rock, in these areas.

negative with an enrichment in the LREE (light rare earth elements), as well as large negative Ce and Eu anomalies. The Eu anomaly, calculated as $Eu_N/\sqrt{(Sm_N*Gd_N)}$, has an average of 0.51. The calculation of the Ce anomaly with the same formula is not applicable in this case, as the La value is probably not reliable due to La contamination and can not be used. This contamination is apparent in the unusually high La peak in the REE diagram. There is a slight difference in the La value between the batches, with the samples from 2004 showing lower values than the samples from 2005. The sample giving a positive trend towards the end of the diagram is JM05MC-19, the specifically sampled section for garnetiferous, leucocratic patches mentioned above. As already discussed the garnet is a good HREE storage mineral and in this case it is apparent that the HREE are enriched in the garnet. As with sample JM05MC-19B, sample JM05MC-19 also does not really represent the whole rock in the area but rather individual parts of it.

4.2. Stable isotopes

The whole rock stable isotope values are very uniform with $\delta^{18}O$ values between 9.8- 10.4. These values are normal values, just on the border between I- and S-type granites (Taylor and Sheppard, 1986). Quartz separates from the above whole rocks gave $\delta^{18}O$ values between 11.2 and 11.9, which are consistent with the whole rock values.

5. DISCUSSION

5.1. Petrology and Mineral chemistry

Petrology and mineral chemistry can be used to investigate the P-T history of the Ramiane Pluton. The first step in this important process is identifying the relative timing of mineral growth and the reaction textures among different minerals. The Ramiane Pluton records a variety of important reaction textures and these can be used to constrain the P-T evolution of the rock, as well as to understand the role of fluids involved in these reactions and the change in oxidation state of the rock. These reaction textures will be discussed below and put in the context of

possible P-T conditions.

The feldspars contribute in the sense that the perthitic texture clearly showing in most of the K-feldspar is formed due to exsolution or replacement in the mineral. The former would suggest a retrograde alteration where a homogenous solid solution in feldspar becomes unstable due to decreased temperature in the rock, and the latter would suggest a sodium enriched liquid reacting with an earlier formed K-feldspar producing the perthite. In this case it appears to be a retrograde exsolution process, as other minerals also appear to show retrograde textures, and as there is no evidence for Na loss in the pluton.

Due to a variety of breakdown textures in the pluton the biotite and amphibole together, are a good source of information for the possible P and T conditions in the rock. Locally, the amphibole appears to be breaking down at the margins to biotite. This is interpreted as a retrograde breakdown texture. Another example of amphibole breakdown textures is the spongy amphibole+quartz+magnetite/hematite textures. The outline of the amphibole breaking down to form the more Si rich amphibole, is that of an euhedral, pyroxene grain. This setting, with the spongy textures and primary euhedral grain shape, is similar to textures observed in pyroxene bearing rocks, (Clemens and Wall, 1984), and indicates that the euhedral shape is probably inherited from igneous pyroxene which broke down to amphibole due to a change in P and T conditions. This initial presence of pyroxene would indicate that the Ramiane Pluton intruded at granulite-facies conditions where pyroxenes are stable. The pyroxenes then subsequently broke down to form euhedral amphiboles. However, there is no evidence, except this textural relationship, of pyroxenes in the samples that has been investigated in this thesis. The areas with spongy texture represent breakdown of the hastingsite, the amphibole formed by the breakdown of pyroxene, to a somewhat compositionally different hastingsite, with related oxides, quartz and feldspars. The breakdown product has an increased Si content and Mg#, as well as decreased Al, Na and to a certain extent, Ti contents. These chemical changes are indicative of an increase in f_{O2}, (Spear, 1993). There is a question of whether the compositional difference between the hastingsites indicates a breakdown from one to a slightly different hastingsite, or if it is merely diffusion occurring in the phase change from pyroxene to amphibole. This relationship has to be further investigated. However, at the moment the petrography favours an interpretation of a breakdown procedure due to the textural relationship between the two amphiboles.

The garnet bearing leucocratic patches are also indicative of a change in environment. There is a noticeable absence of amphibole, biotite and oxides around the garnet clusters, resulting in leucocratic halos. This indicates that amphibole and biotite are reacting to produce almandine garnet, with the excess Si, K, Na and Ca generating quartz and feldspars. This could imply a prograde breakdown procedure as the garnet P and T stability fields primarily lies above that of the amphibole and the biotite. However, put into a larger context of the Ramiane P-T-history, a prograde breakdown does not appear to be the most likely turn of events. The presence of fluid inclusions in the garnet and quartz rather indicate a retrograde reaction involving mobilised fluids from the intrusive event. This process would rather then be a retrograde, fluid influenced, biotite and amphibole breakdown to form garnet. The presence of fluids, increases the f_{O2} and thus yields an oxidation environment. The high percentage of andradite in the garnet

Table 3. P-T calculations made by use of THERMOCALC, based on mineral data from the Ramiane Pluton.

Sample No.	17X (a)		17X (b)		20 (a)		20 (b)	
P and T	**T (°C)**	**P (kBar)**	**T (°C)**	**P (kBar)**	**T (°C)**	**P (kBar)**	**T (°C)**	**P (kBar)**
Fluid bearing								
aH_2O= 1.0	756± 59	10.1± 1.3	735± 58	9.9± 1.2	733± 69	9.1± 1.2	826± 79	8.2± 1.3
aH_2O= 0.8	—	—	716± 54	9.5± 1.2	714± 65	8.8± 1.2	801± 74	7.8± 1.3
aH_2O= 0.7	727± 54	9.6± 1.2	—	—	—	—	—	—
aH_2O= 0.6	—	—	699± 51	9.2± 1.2	—	—	—	—
aH_2O= 0.5	—	—	—	—	687± 59	8.3± 1.2	761± 66	7.2± 1.3
aH_2O= 0.4	689± 47	8.9± 1.2	673± 47	8.7± 1.2	—	—	—	—
aH_2O= 0.2	634± 41	7.9± 1.2	620± 40	7.7± 1.2	624± 48	7.1± 1.2	677± 50	6± 1.3
aH_2O= 0.1	578± 35	6.8± 1.1	566± 34	6.7± 1.1	572± 41	6.1± 1.2	—	—
Non- Fluid bearing								
aH_2O= 1.0	756± 59	10.1± 1.3	735± 58	9.9± 1.2	733± 69	9.1± 1.2	826± 79	8.2± 1.3
aH_2O= 0.8	726± 55	9.6± 1.2	707± 54	9.3± 1.2	—	—	—	—
aH_2O= 0.6	691± 51	8.9± 1.2	673 ± 50	8.7± 1.2	—	—	—	—
aH_2O= 0.5	—	—	—	—	657± 57	7.7± 1.2	726± 63	6.7± 1.2
aH_2O= 0.4	646± 46	8.1± 1.1	630± 45	7.9± 1.1	—	—	—	—
aH_2O= 0.2	578± 39	6.8± 1.1	565± 38	6.7± 1.1	575± 46	6.1± 1.1	625± 48	5.2± 1.1
aH_2O= 0.1	521± 33	5.8± 1.0	510± 33	5.7± 1.0	533± 40	5.2± 1.0	—	—

Note: aH_2O= water activity, P= Pressure, T=Temperature, (a) differs from (b) in change of mineral data from within the sample

is indicative of oxidisation as andradite favours Fe^{3+}. However the Droop, (1987), recalculation of the Fe^{3+} may in this case have overestimated the Fe^{3+} which can be seen in the appendix for mineral data, and it can not be entirely ruled out that there might be a complication with the recalculation since the formula does not consider the amount of Al in the mineral. However, it is also possible that the EDS data gives a higher value for FeO then necessary, due to wrong valence setting, and after being normalised the overestimation of the Fe^{3+} is apparent. The garnet appears to be slightly un-stoichiometric with regards to the M- and A-sites, and this is due to an original small excess of cations. The garnet is normally a relatively stoichiometric mineral and therefore a large part of the excess Fe^{3+} on the M-site needs to fill out the A-site, however not all of it. It is important to know that the Fe^{3+} in the garnet from the Ramiane Pluton is somewhat overestimated.

5.2. P-T- modelling

Modelling of the P and T conditions in the Ramiane Pluton is based on the garnet bearing patches. However, it should be noted that the garnet bearing patches are not representing the entire pluton, but rather an event that occurred locally in the fluid enriched patches, later in the cooling stage of the pluton. When trying to model P-T conditions for this garnet-forming event, the composition of the fluid had a strong influence on the P-T results. P-T conditions were calculated assuming two different scenarios. The one case was calculated on a fluid-absent rock and the other on a fluid-present rock (Table 3). The best results, based on smallest P and T variations, were obtained for a fluid present intrusive rock with a water activity (aH_2O) of 0.1-0.2, or a fluid absent rock with a fixed aH_2O of 0.1-0.2. Alkaline rocks are often found associated with fluids (Potter, Rankin and Treloar, 2004, Santos and Clayton, 1995, Bi, Cornell and Hu, 2002),

and petrological studies of the Ramiane Pluton have shown abundant fluid inclusions in the garnet and quartz that supports this fluid-rich hypothesis. The breakdown of amphibole as a result of increased f_{O2} also supports a fluid-rich scenario.

In the situation of a fluid present intrusive rock, P-T calculations using THERMOCALC (Holland and Powell, 1998) yield average temperatures and pressures of 639°C ± 45°C, 7.2 kBar ± 1.2 kBar for an aH_2O of 0.2, and 572°C ± 37°C and 6.5 kBar ± 1.1 kBar for an aH_2O of 0.1. However, if the rock was fluid absent with a fixed aH_2O of 0.2-0.1, the average pressure and temperatures would be lower and in the range of 554°C ± 39°C and 5.9 kBar ± 1.1 kBar. As mentioned before the issue of the presence or absence of a fluid phase is important due to the strong influence it has on the P-T results. The error of the P and T calculations also increases proportionally, which makes it very difficult to determine the true P and T when the garnet was formed. Using the data with the lower aH_2O it would appear as if the T of the garnet forming event in the patches is around 600°C at P of between 6 and 7 kBars. This would represent the amphibolite facies and thus show a cooling stage in the P-T-history of the pluton, if assumed that when it intruded it was a pyroxene bearing rock, and subsequently yielding granulite facies minral assemblages (Fig.20).

Figure 20. Metamorphic facies diagram from Yardley, (1989)

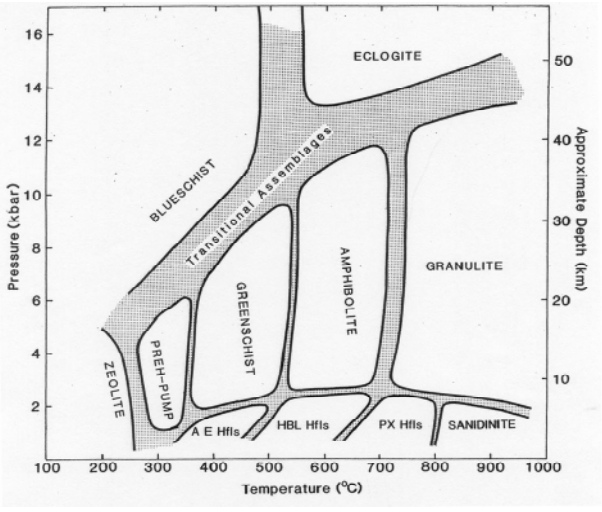

5.3. Possible protolith and its mechanical evolution

The aim of the modelling was to establish whether there is a possible protolith among the surrounding rocks for the Ramiane Pluton, and thus whether the pluton is an *in situ* intrusion or not. The attempt to model a possible protolith and investigate its possible mechanical evolution has been semi-successful. It did not identify a possible protolith among the rocks from the surrounding area, though it did put some constraints on the material the Ramiane could have originated from. Some of the mechanical evolution has also been unravelled. Using similar methods to Martin, (1987), various trace elements were plotted vs SiO_2 to determine the compatibility of the elements in the Ramiane Pluton. This proved to be quite difficult and only a few elements showed clear patterns. The fact that many of the plots show very scattered patterns and that for example the Zr/ Nb vs SiO_2 does not really show any trend could be a reflection of the original protolith conditions. Also, the Rb vs Sr shows a clear trend but the actual ppm values are different from the surrounding rocks. The Rb has higher values and the Sr has lower values. This is indicative of a less evolved protolith than the surrounding rocks, as the Rb is incompatible and the Sr is compatible in reference to each other. With the elements that did show a trend such as Sr, Rb, Zr and Ba, binary log/ log diagrams with compatible vs incompatible elements were created to determine if the rock had undergone partial melting or fractionation. A steep slope would indicate fractionation, and

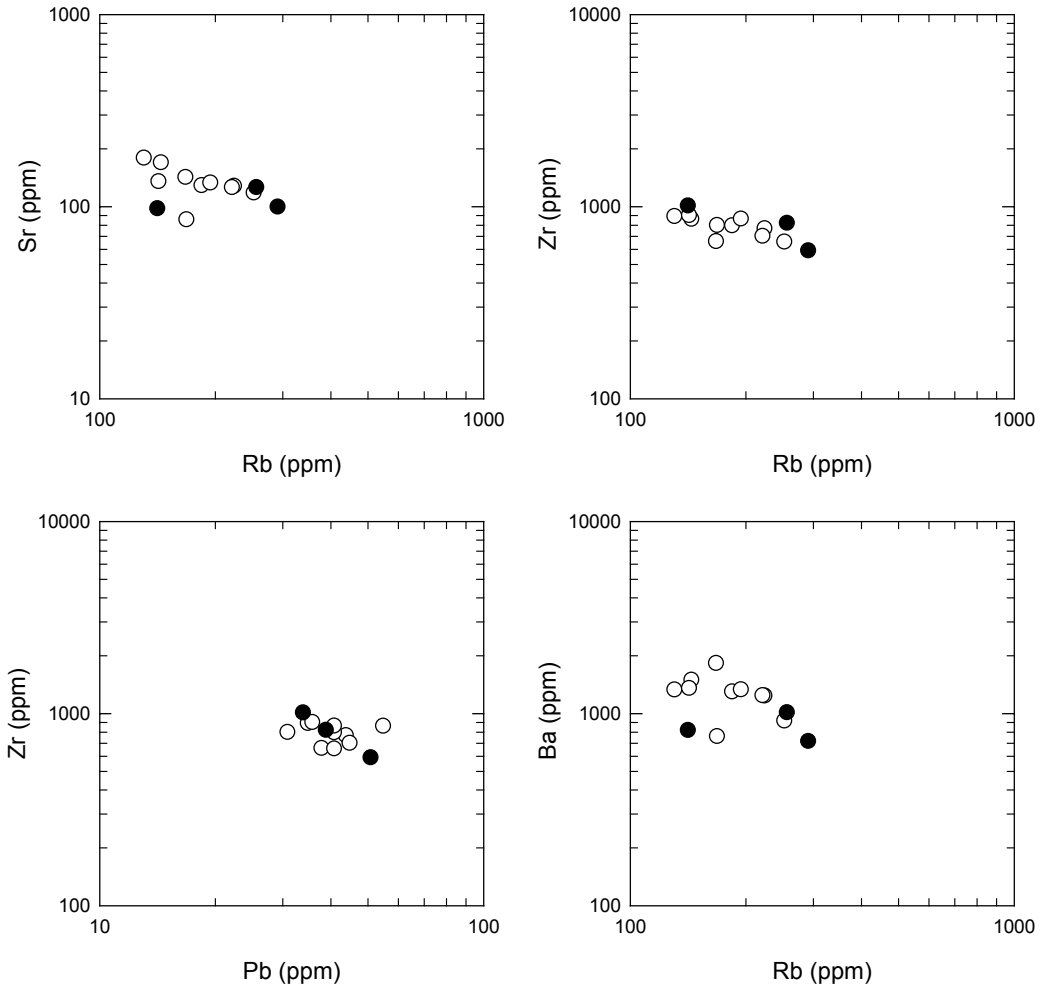

Figure 21. The binary log/ log diagrams showing the relatively shallow sloping trends of the elements. This suggests a partial melting of the rock and not a fractionation

a more gentle slope, partial melting (Martin, 1987, Fig. 21). It is clear from Fig. 21 that the rock has not undergone any significant degree of fractionation. However a difficulty in assuming partial melting or not in the pluton is the fact that it is a pluton and hence must melt and crystallise and thus undergo partial melting. Minerals such as ilmenite, ortho- and clino- pyroxenes and plagioclase from granulite facies rocks were used to model the protolith composition. The reason for using granulite facies minerals was based on the surrounding metamorphic grades as well as petrological investigations which indicate that pyroxene was part of the early mineral assemblage in the Ramiane Pluton. (Fig. 22).

The minerals were then plotted together with the samples and thus formed a polygon where they would coexist with each other. The trend line for the samples goes through the coexisting polygon and the place where it enters and exits the polygon indicates the maximum and minimum values within which the element must lie in order to be a possible protolith of the Ramiane Pluton. Each of the elements were put into a table and normalised. Then the trial and error procedure of making them all fit together within respective values was carried out. Eventually there was a reasonable match that seemed to be a valid protolith for the Ramiane Pluton. It turns out that neither the Rapale nor the Metacheria rocks are good matches for the hypothetical protolith. However, out of the two different rock types it appears as the Rapale Gneiss of the Nampula Subprovince is closer in composition to being a possible protolith than

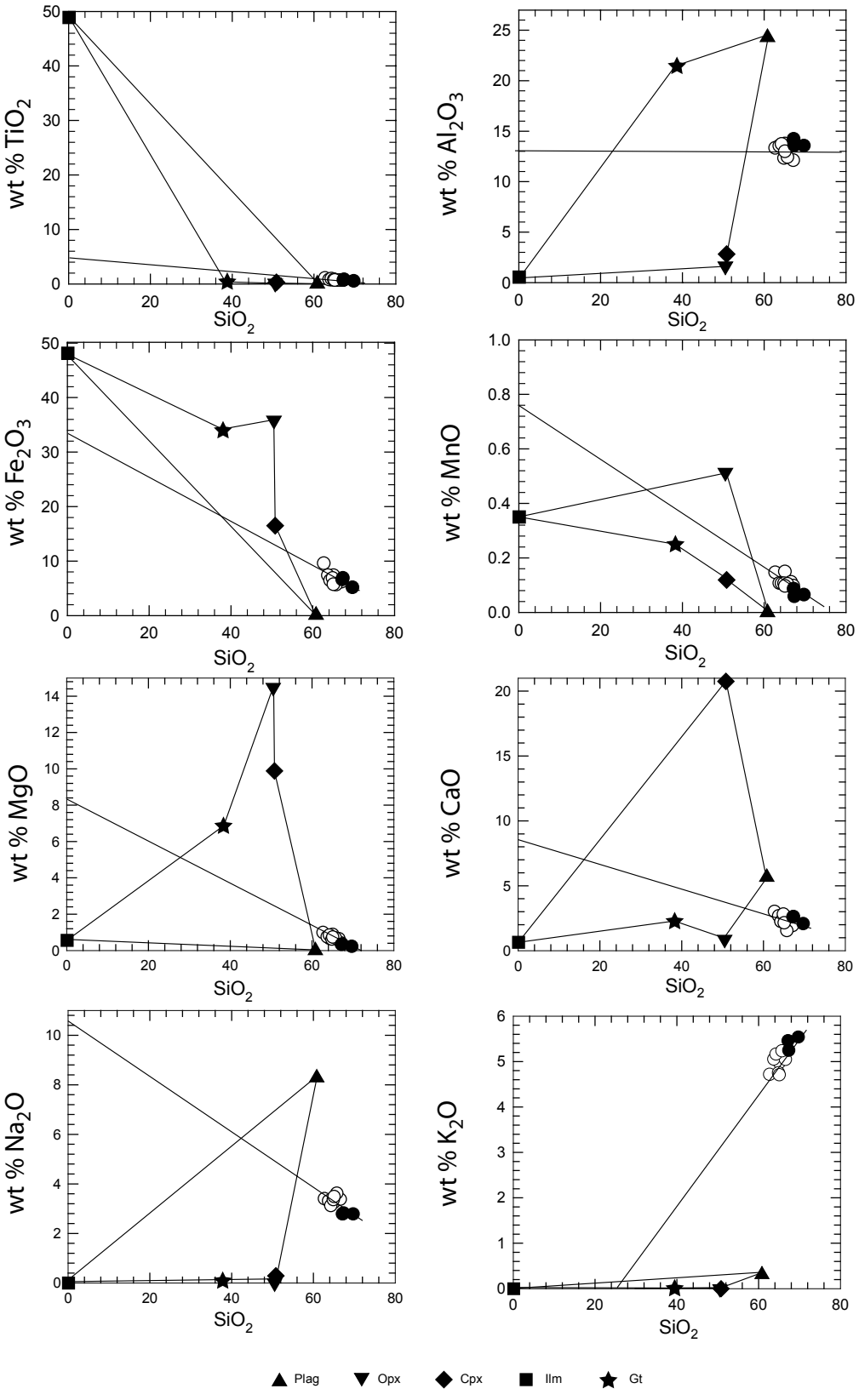

Figure 22. Harker diagrams showing fields of coexisting minerals and projection of trend line used to estimate original protolith compositional ranges.

the Metacheria basement rocks. The testing of the possible protolith was carried out with the use of the formula $C_L = C_0 / D + F (1-D)$ where C_L= Part of rock that is liquid, C_0= Original source rock, $D = (C_{Solid} / C_{Liquid})$ = Bulk repartition coefficient, F= Melt fractions. The F was given several different values (0-25%), the D values were taken from granitic melts as well as from the mineral proportion that was created during the modelling, (Rollinson, 1993). The initial C_0 was created by an average ppm value from the Rapale and the Metacheria rocks separately, to be able to investigate if the one was a better match than the other. These were from there on treated separately in regards to the comparison with the modelled protolith. The zircon values had to be very high in both the assumed rocks to be able to correlate to the modelled protolith, and the high Ba contents were also a constant issue of problem, as well as K. As mentioned earlier, the SiO_2 vs Ba diagram suggests K-feldspar in the protolith, and it would appear as if that assumption is valid, as there were difficulties to get a high enough Ba ppm value. However, the large amount of K-feldspar needed to satisfy the Ba excess would be inconsistent with the used rock composition. K, as opposed to every other major element, has a positive trend. This is also similar to the K trend in Martin, (1987). However, in the case of the Ramiane Pluton the K trend line goes below zero which indicates a loss in K. This in turn would imply that the rock was not a closed system and thus that the modelling is not applicable due to the variable loss and gain of different elements. However, in that situation, the loss of equally mobile Na should also appear as a positive trend with a corresponding negative value for the trend intercept which it does not. The choice of minerals for the modelling of a possible protolith is important, and can change the protolith composition. In this example K-feldspar would have been needed to a larger extent instead of plagioclase in the modelled source rock to get the Ba content balanced. However, that in turn would have brought up the Al content in the modelled protolith and lowered the already very low Na out of the limits for coexistence with the other minerals.

The theory behind the construction of a possible source rock is relatively straight forward but the actual use of it is somewhat limited due to the assumptions that have to be made before plotting and interpreting can be carried out. In this case it was initially assumed that the system was closed, and it now appears as if this assumption might not be valid and then it is very hard to model a protolith. One could possibly argue that the halo of higher radiometric signal, possible due to K mobilisation, surrounding the Ramiane could have suggested that this was an open system, and thus modelling would not have had to be attempted. The implications of this possible open system on other parts of the project is not entirely clear, but any event that change the original composition of the pluton ought to have some influence on the work carried out on it. However, to what extent this open system has changed the Ramiane Pluton composition is unclear at the moment. For example the stable isotope studies show no sign of a metasomatic event and thus are implying that the system has not been influenced by a metasomatic event to a larger extent. However, this may also need more investigations

5.4. Geochronology

To be able to locate the intrusive event in the regional geology history and time there has to be made an age analyses, in this case SHRIMP U-Pb data. It is not enough with relative data ages, such as the Ramiane Pluton intruding into

the Metacheria Metamorphic Complex. The SHRIMP U-Pb ages for the Ramiane Pluton suggest an intrusive age of 636.8 ± 5.3 Ma and a possible metamorphic event, or as I believe a cooling age of 596 ± 5 Ma. This appears to be highly probable and there are other 640 Ma ages available for correlation within the structure, such as the sheared TTG gneisses of the Culicui Suite, as well as rocks north of the Lurio Belt. These ages clearly suggest a geological event in the Pan-African time, though the Culicui have intrusive ages from the Kibaran age and that is something that the Ramiane Pluton does not have. It appears as if many of the ages from the Nampula Subprovince that surrounds the Monapo Structure also have ages from the Kibaran. However, many record a metamorphic event between 600-500 Ma. The SHRIMP data from the Ramiane Pluton appears to be very straight forward. However, the problem arises when the data from the Metacheria Metamorphic Complex is put into the equation. This is the assumed basement rock the Ramiane has intruded into. The ages of 634 ± 8 Ma and 579 ± 11 Ma were the results of the SHRIMP U-Pb data. This would imply that the Ramiane is older than the rocks it intrudes into. However, considering the overlap in age range it is still possible that the Metacheria rocks were emplaced first. This appears to be the case, due to the occurrence of clasts of Metacheria rocks within the Ramiane Pluton, which is clear evidence of their relative ages (Fig. 8). The younger age obtained from the Metacheria Metamorphic Complex is closer related in age to the metamorphic event of the Culicui Suite than the younger age of the Ramiane that appears to have an earlier P-T event that does not show up in the Metacheria SHRIMP data. The younger age suggested for the Ramiane Pluton by SHRIMP U-Pb data also has a correlation within the structure. The younger Evate Carbonatite appears to have an age of approximately 590 Ma as well (Siegfried, 1999). However, the connection between the ages from these two rock types is still unknown to me. There is only one data set for each of the Ramiane and the Metacheria suites, so for clarification it would be rewarding to have more data to compare with. There is, for example, no available age of the Mazerapane Suite. Maybe the lack of P-T event in the Metacheria in 596 ± 5 Ma is a sign of a metasomatic event in the Ramiane at this time. This would then give raise to the radiometric halo around the Ramiane Pluton. The area from where the dated Metacheria sample was taken from is located approximately 30 km from the pluton, and thus would not have to be affected by a metasomatic Ramiane event. It would be interesting to have an age from the Metacheria nearby the Ramiane Pluton, to compare with as well. There are a lot of age data about to be available shortly and they will surely shed some light on many of the age related questions still unanswered in this thesis.

6. CONCLUSIONS

The known history of the alkaline granites and the syenodiorite of the Ramiane Pluton started with the intrusion of the A- type Ramiane Pluton at 636.8 ± 5.3 Ma. It intruded into the Metacheria Metamorphic Complex, 634 ± 8 Ma. This is difficult to argue only based on the SHRIMP ages, however, clasts of the Metacheria basement within the Ramiane Pluton supports the relative ages of the two rocks.

The composition of the Ramiane Pluton shows evidence of a relatively juvenile protolith. This is implied by the Rb and Sr values from the Ramiane Pluton, as well as from the surrounding rocks. The Ramiane has higher Rb values and lower Sr values and thus do

not appear to have the same protolith as the surrounding Metacheria Metamorphic Complex and the Nampula Subprovince. It also does not appear as if a possible metasomatic event of the Ramiane could have altered the values compared to the surrounding rocks. The Rb would then get a lower ppm value in the pluton due to its mobility. If that has been the case it would only support the hypothesis that the Ramiane is less evolved than the surrounding rocks, as the Ramiane Rb value would have been even higher in comparison with the other rocks. The same process would also have increased the Sr in the rock and clearly it did not. If it did, the value was already very low, and as in the case of Rb this would only support the less evolved protolith hypothesis of the Ramiane Pluton.

Due to the assumed presence of pyroxenes in the pluton the intrusion P and T was in the granulite-facies range. The author has not been able to locate any of these pyroxenes in the rock. However, this is a result expected since the rock has cooled down to the point where pyroxenes are no longer stable. The Ramiane Pluton also shows evidence for having been rich in fluids. There are abundant fluid inclusions in garnet and quartz in the Ramiane Pluton, as appears to be the case of many alkaline intrusive rocks and complexes (Potter, Rankin and Treloar, 2004, Santos and Clayton, 1995, Bi, Cornell and Hu, 2002).

The younger SHRIMP age of the Ramiane Pluton of 596 ± 5 Ma, represents part of a cooling phase of the Ramiane Pluton. As mentioned before in the text the loss of K in the pluton may be evidence for a metasomatic event which yielded a halo around the Ramiane that has a high radiometric signal. Due to the loss of K in the rock I assume much of the fluids that originally came with the Ramiane Pluton have been transported out of the pluton. It is difficult to know whether this possible metasomatic event is intrusion related, or if it is represented by the age 596 ± 5 Ma. The breakdown of amphiboles and biotite to garnet in the Ramiane Pluton is indicative of relatively high temperature and pressure conditions. The assumption is that the garnet grew during an oxidation event on the behalf of amphibole and biotite in left over fluid patches after most of the fluids had mobilised outside the pluton. The environment created in these patches due to increase in f_{O2} favoured an oxidation event. Evidence for this is the products in the area of spongy breakdown textures earlier discussed in the text. This oxidation event would also explain the amount of andradite in the garnet as more Fe^{3+} became available. The P and T calculated for this event suggest a T for forming of garnet, ~600°C and P of 6-7 kBars. This is relatively low but not unlikely. These values are based on the THERMOCALC results that may not be valid, due to the unknown influence of the fluid in the rock. Since the oxidation event that occurred at the same time as garnet was formed, there has been breakdown of amphibole to biotite on the amphibole margins and formation of perthite. Both of these are retrograde processes and the breakdown from amphibole to biotite would occur at lower T than the stability field of garnet as now is the case.

There have been activities in the Monapo Structure after the oxidation event, such as the possible metamorphic event of the surrounding Metacheria Metamorphic Complex, however there are no textural or chemical evidence for any larger event such as the one at 596 ± 5 Ma in the Ramiane Pluton.

7. ACKNOWLEDGEMENTS

First and foremost I would like to thank Dr Jodie

A. Miller for being my supervisor at Stellenbosch University. Her support, encouragements and faith in my abilities have been incredibly valuable to me. Thank you for all the hard work you put in. A mutual appreciation of ammonium chloride, aka salmiak, helped us getting along even better. To Dr Paul Macey at the Council for Geosciences, for doing all the hard work out in the field and for providing me with much valuable information. (3 hours for a rock sample is nothing, and we **do** want good samples!) Thank you for always helping out whenever I was in need, even though you were swamped. Without Paul and Jodie there wouldn't have been a Monapo Structure Master thesis. To the Council for Geosciences for letting me use their data. To Professor Alex Kisters for letting me ambush him occasionally with a hundred strange questions at a time and whenever structures were involved. To Professor Gary Stevens for taking time with questions. To Professor Anders Lindh for being my supervisor at basecamp, Lund University and for never being a stranger when it comes to answering questions, and giving support. To Professor John Clemens for valuable opinions. To Esmé Spicer, Stefan Kruger and Riana Rossouw for all their help with any kind of technical aspect of my work. That is when we actually had access to power… To Jean François Moyen for help with my chemical data, to Dr Riana van den Bergh for always offering to help out whenever I was in doubt. To Robert Ward and Arnaud Villaros for always being in my corner. Without you guys I don't know what I would have done. Well, I guess there is ONE thing I know I wouldn't have done…. To Andrea King and Stephan Fourie for helping out with preparations.

8. LIST OF REFERENCES

Bi, X., Cornell, D., H., Hu, R.,2002. REE composition of primary and altered feldspar from the mineralized alteration zone of alkaline intrusive rocks, western Yunnan Province, China. *Ore Geology Reviews* Vol 19, 68-78.

Borthwick, J. and Harmon, R.S., 1982. A note regarding ClF3 as an alternative to BrF5 for oxygen isotope analysis. *Geochimica et Cosmochimica Acta*, Vol 46, 1665-1668.

Clayton, R.N. and Mayeda, T.K., 1963. The use of bromine pentafluoride in the extraction of oxygen from oxides and silicates for isotopic analysis. *Geochimica et Cosmochimica Acta,* Vol 27, 43-52.

Clemens, J., D. and Wall, V., J., 1984. Origin and evolution of a peraluminous ignimbrite suite: the Violet Town Volcanics. *Contributions to Mineralogy and Petrology* 88, 354-371.

Coplen, T.B., Kendall, C. and Hopple, J., 1983. Comparison of stable isotope reference samples. *Nature*, 302, 236-238.

Coplen, T.B., 1993. Normalisation of oxygen and hydrogen isotope data. *Chemical Geology*, 72, 293-297.

Cox, K. G., Bell, J. D., Pankhurst, R. J., 1979. *The interpretation of igneous rocks*. George Allen and Unwin, London.

Debon, R., Lefort, P., 1983. A chemical mineralogical classification of common plutonic rocks. *Earth Science* 73, 135-149.

Deer, W., A., Howie, R., A. and Zussman, J, 1992. *An introduction to the rock forming minerals*. Pearson Education Limited, England.

Droop, G. T. R., 1987. A general equation for estimating Fe3+ concentrations in ferromagnesian silicates and oxides from microprobe analyses, using stoichiometric criteria. *Mineralogical Magazine* Vol 51, 431-435.

Eby, G. Nelson., 1990. The A- type granitoids: A review of their occurrence and chemical characteristics and speculations on their petrogenesis. *Lithos* Vol 26, 115- 134.

Grantham, G., H., Maboko, M., Eglington, B., M., 2003. A review of the evolution of the Mozambique Belt and implications for the amalgamation and dispersal of Rodinia and Gondwana. In: Yoshida, M., Windley, B., F. and Dasgupta, S., (eds). *Proterozoic East Gondwana: Supercontinent Assembly and Breakup,* Geological Society London Special Publications 206, 401- 425.

Groenewald, P., B., Moyes, A., B., Grantham., G., H., Krynauw, J., R., 1995. East Antarctic crustal evolution: geological constraints and modelling in western Dronning Maud Land. *Precambrian Research* 75, 231-250.

Holland, T., J., B., Powell, R., 1998. An internally consistent thermodynamic dataset for phases of petrological interest, *Journal of Metamorphic Geology*, 16, 309-343.

Martin, Hervé, 1987. Petrogenesis of Archaean Trondhjemites, Tonalites and Granodiorites from Eastern Finland: Major and Trace Element Chemistry. *Journal of Petrology* Vol 28, 921-953.

Macey, P., H., Miller, J., A., Siegfried, P., Karlsson, J., Grantham, G., H., 2006. *A new lithostratographic subdivision of the rocks of the Monapo Structure, Northeastern Mozambique*. Abstract, CAG 21, Maputo 3-5 th of July, 2006.

McCrea, J.M., 1950. On the isotopic chemistry of carbonates and a palaeotemperature scale. *Journal of Chemical Physics*, 18, 849-857.

Kröner, A., Sacchi, R., Jaeckel, P. and Costa, M., 1997. Kibaran magmatism and Pan-African granulite metamorphism in northern Mozambique: single zircon ages and regional implications. *Journal of African Earth Sciences* Vol 25, 467- 484.

Kröner, A., 1991. African linkage of Precambrian Sri Lanka. *Geologische Rundschau* 80/2.

Leake, B., E *et al*, 1997. Nomenclature of Amphiboles: Report of the Subcommittee on Amphiboles of the International Mineralogical Association Commission on New Minerals and Mineral Names, 1997. *Mineralogical Magazine* Vol 61, 295- 321.

Pinna, P., Jourde, G., Calvez, J. Y., and Marques, J. M., 1993. The Mozambique Belt in northern Mozambique: Neoproterozoic (1100- 850 Ma) crustal growth and tectogenesis, and superimposed Pan-African (800- 550 Ma) tectonism. *Precambrian Research* 62, 1-59.

Potter, J., Rankin, A., H., and Treloar, P., J., 2004. Abiogenic Fischer-Tropsch synthesis of hydrocarbons in alkaline igneous rocks; fluid inclusion, textural and isotopic evidence from the Lovozero Complex, N.W. Russia. *Lithos* Vol 75, 311-330.

Rollinson, H., 1993. *Using geochemical data: evaluation, presentation, interpretation.* Pearson Education Limited, England.

Sacchi, R., Cadoppi, P. and Costa, M., 2000. Pan-African reactivation of the Lurio segment of the Kibaran Belt system: a reappraisal from recent age determinations in northern Mozambique. J*ournal of African Earth Sciences* Vol 30, 629- 639.

Santos, R., V. and Clayton, R., N., 1995. Variation of oxygen and carbon isotopes in carbonatites: A study of Brazilian alkaline complexes. *Geochimica et Cosmochimica Acta,* Vol 59, 1339-1352.

Siegfried, P., A., 1999. The Monapo structure and intrusive complex- An example of large-scale alkaline metasomatism in northern Mozambique. Mineral Deposits: *Processes to Processing*, 683-686.

Spear, Frank., S., 1993. *Metamorphic Phase Equilibria and Pressure-Temperature-Time Paths*, Mineralogical Society of America.

Sun, S., S., and McDonough, W., F., 1989. Chemical and isotopic systematics of oceanic basalts: implications for mantle composition and processes. In: Saunders, A., D., and Norry, M., J., (eds.) *Magmatism in ocean basins* Geological Society London Special Publication 42, 313- 345.

Taylor, H., P., Jr. and Sheppard, S., M., F., 1986. In: Valley, J., W., Taylor, H., P., Jr. and O'Neil, J., R., (eds) Stable Isotopes in high temperature geological processes,

Mineralogical Society of America, *Reviews in Mineralogy* Vol 16, 227- 271.

Venneman, T.W., and O'Neil, J.R., 1993. A simple and inexpensive method of hydrogen isotope and water analyses of minerals and rocks based on zinc reagent. *Chemical Geology (Isotope Geoscience)*, 103, 227-234.

Viola, G., Henderson, I., Bingen, B., Feitio, P., Thomas, R., Hollick, L and Jacobs, J. 2006. *A new tectonic framework for northern Mozambique,* Abstract CAG 21, Maputo 3-5 th July, 2006.

Whalen, J., B., Currie, K., L., and Chappell, B., W., 1987. A- type granites: Geochemical characteristics, discrimination and petrogenesis: *Contributions to Mineralogy and Petrology* Vol 95, 407- 419.

Wilson, M., 1989, *Igneous petrogenesis- A Global tectonic approach*. Chapman and Hall, London

Yardley, B., W., D., 1989. *An introduction to metamorphic petrology*. Longman Scientific and Technical, England.

Tidigare skrifter i serien "Examensarbeten i Geologi vid Lunds Universitet":

151. Jonsson, Henrik, 2002: Permeability variation in a tidal Jurassic deposit, Höganäs basin, Fennoscandian Border Zone
152. Lundgren, Anders, 2002: Seveskollorna i nord-östra Kebnekaise, Kaledoniderna: metabasiter, graniter och ögongnejser.
153. Sultan, Lina, 2002: Reconstruction of fan-shaped outwash in front of the Mýrdalsjökull ice cap, Iceland: Architecture and style of sedimentation.
154. Rimša, Andrius, 2002: Petrological study of the metamafic rocks across the Småland-Blekinge Deformation Zone
155. Lund, Magnus, 2002: Anti-slope scarp investigation at Handcar Peak, British Columbia, Canada.
156. Sjöstrand, Lisa: 2003: Early to early Middle Ordovician conodont biostratigraphy of the Tamsalu drill core, central Estonia.
157. Nilsson, Jonas, 2003: Carcharhiniforma hajar från Limhamns kalkbrott.
158. Larsson, Linda M., 2003: Late Triassic and Early Jurassic palynology of the Höganäs Basin and the Ängelholm Trough, NW Scania, Sweden.
159. Sköld, Pia, 2003: Holocen skogshistoria i Stenshuvuds nationalpark, Skånes östra kust, Sverige.
160. Fuchs, M., 2003: Påverkan av sterilisering på gruvsand – en mineralogisk och texturell undersökning.
161. Ljungberg, Julia, 2003. Sierggavággeskollan i gränslandet mellan Sarek och Padjelanta; miljöindikatorer för fjällkedjeberggrundens bildning.
162. Håkansson, Lena, 2003: An architectural element analysis of a large-scale thrust complex, Kanin Peninsula, NW Russia: interaction between the Barents and Kara Sea ice sheets.
163. Davidson, Anja, 2003: Ignimbritenheterna i Barranco de Tiritaña, övre Mogánformationen, Gran Canaria.
164. Näsström, Helena, 2003: Klotdioriten vid Slättemossa, centrala Småland – mineralkemi och genes.
165. Nilsson, Andreas, 2003: Early Ludlow (Silurian) graptolites from Skåne, southern Sweden.
166. Dou, Marion, 2003: Les ferromagnésiens du granite rapakivique de Nordingrå – centre-est de la Suède – composition chimique et stade final de cristallisation.
167. Jönsson, Emma, 2003: En pollenanalytisk studie av råhumusprofiler från Säröhalvön i norra Halland.
168. Alwmark, Carl, 2003: Magmatisk och metamorf petrologi av en mafisk intrusion i Mylonitzonen.
169. Pettersson, Ann, 2003: Jämförande litologisk och geokemisk studie av Sevens amfibolitkomplex i Sylarna och Kebnekaise.
170. Axelsson, Katarina, 2004: Bedömning av potentiell föroreningsspridning från ett avfallsupplag utanför Löddeköpinge, Skåne.
171. Ekestubbe, Jonas, 2004: $^{40}Ar/^{39}Ar$ geokronologi och implikationer för tolkningen av den Kaledoniska utvecklingen i Kebnekaise.
172. Lindgren, Paula, 2004. Tre sensvekofenniska graniter: kontakt- och åldersrelationer samt förekomst av metasedimentära enklaver.
173. Janson, Charlotta, 2004. A petrographical and geochemical study of granitoids from the south-eastern part of the Linderödsåsen Horst, Skåne.
174. Jonsson, Sara, 2004: Structural control of fine-grained granite dykes at the Äspö Hard Rock Laboratory, north of Oskarshamn, Sweden.
175. Ljungberg, Carina, 2004: Belemniters stabila isotopsammansättning: paleomiljöns och diagenesens betydelse.
176. Oster, Jessica, 2004: A stratigraphic study of a coastal section through a Late Weichselian kettle hole basin at Ålabodarna, western Skåne, Sweden.
177. Einarsson, Elisabeth, 2004: Morphological and functional differences between rhamphorhynchoid and pterodactyloid pterosaurs with emphasis on flight.
178. Anell, Ingrid, 2004: Subsidence in rift zones; Analyzing results from repeated precision leveling of the Vogar Profile on the Reykjanes Peninsula, Southwest Iceland.
179. Wall, Torbjörn, 2004: Magnetic grain-size analyses of Holocene sediments in the

North Atlantic and Norwegian Sea – palaeoceano-graphic applications.

180. Mellgren, Johanna, S., 2005: A model of reconstruction for the oral apparatus of the Ordovician conodont genus *Proto-panderodus* Lindström, 1971.
181. Jansson, Cecilia, 2005: Krossbergskvalitet och petrografi i den kambriska Harde-bergasandstenen i Skåne.
182. Öst, Jan-Olof, 2005: En övergripande beskrivning av malmbildande processer med detaljstudier av en bandad järnmalm från södra Dalarna, Bergslagen.
183. Bragée, Petra, 2005: A palaeoecological study of Holocene lake sediments above the highest shoreline in the province of Västerbotten, northeast Sweden.
184. Larsson, Peter, 2005: Palynofacies och mineralogi över krita-paleogengränsen vid Stevns Klint och Kjølby Gaard, Danmark.
185. Åberg, Lina, 2005: Metamorphic study of metasediment from the Kangilinaaq Peninsula, West Greenland.
186. Sidgren, Ann-Sofie, 2005: $^{40}Ar/^{39}Ar$-geokronologi i det Rinkiska bältet, västra Grönland.
187. Gustavsson, Lena, 2005: The Late Silurian Lau Event and brachiopods from Gotland, Sweden.
188. Nilsson, Eva K., 2005: Extinctions and faunal turnovers of early vertebrates during the Late Silurian Lau Event, Gotland, Sweden.
189. Czarniecka, Ursula, 2005: Investigations of infiltration basins at the Vomb Water Plant – a study of possible causes of reduced infiltration capacity.
190. G³owacka, Ma³gorzata, 2005: Soil and groundwater contamination with gasoline and diesel oil. Assessment of subsurface hydrocarbon contamination resulting from a fuel release from an underground storage tank in Vanstad, Skåne, Sweden.
191. Wennerberg, Hans, 2005: A study of early Holocene climate changes in Småland, Sweden, with focus on the '8.2 kyr event'.
192. Nolvi, Maria & Thorelli, Gunilla, 2006: Extraterrestrisk och terrestrisk kromrik spinell i fanerozoiska kondenserade sediment.
193. Nilsson, Andreas, 2006: Palaeomagnetic secular variations in the varved sediments of Lake Goœci¹¿, Poland: testing the stability of the natural remanent magnetization and validity of relative palaeo-intensity estimates.
194. Nilsson, Anders, 2006: Limnological responses to late Holocene permafrost dynamics at the Stordalen mire, Abisko, northern Sweden.
195. Nilsson, Susanne, 2006: Sedimentary facies and fauna of the Late Silurian Bjärsjö-lagård Limestone Member (Klinta Formation), Skåne, Sweden.
196. Sköld, Eva, 2006: Kulturlandskapets förändringar inom röjningsröseområdet Yttra Berg, Halland - en pollenanalytisk undersökning av de senaste 5000 åren.
197. Göransson, Ammy, 2006: Lokala miljöförändringar i samband med en plötslig havsyteförändring ca 8200 år före nutid vid Kalvöviken i centrala Blekinge.
198. Brunzell, Anna, 2006: Geofysiska mätningar och visualisering för bedömning av heterogeniteters utbredning i en isälvsavlagring med betydelse för grundvattenflöde.
199. Erlfeldt, Åsa, 2006: Brachiopod faunal dynamics during the Silurian Ireviken Event, Gotland, Sweden.
200. Vollert, Victoria, 2006: Petrografisk och geokemisk karaktärisering av metabasiter i Herrestadsområdet, Småland.
201. Rasmussen, Karin, 2006: En provenans-studie av Kågerödformationen i NV Skåne – tungmineral och petrografi.
202. Karlsson, Jonnina, P., 2006: An investigation of the Felsic Ramiane Pluton, in the Monapo Structure, Northern Moçambique.

LUNDS UNIVERSITET

Geologiska institutionen
Gentrum för GeoBiosfärsvetenskap
Sölvegatan 12, 223 62 Lund